Submitted, accepted and published by
Chemical Engineering Science 66 (2011) 689-702

# KINETICS OF REDOX REACTIONS OF ILMENITE FOR CHEMICAL-LOOPING COMBUSTION

Alberto Abad*, Juan Adánez, Ana Cuadrat, Francisco García-Labiano, Pilar Gayán, and Luis F. de Diego

Department of Energy and Environment, Instituto de Carboquímica (CSIC),
Miguel Luesma Castán 4, 50018 Zaragoza, Spain

## Abstract

The objective of this study was to establish the kinetic of both reduction and oxidation reactions taking place in the Chemical-Looping Combustion (CLC) process using ilmenite as oxygen carrier. Because of the beneficial of the use of pre-oxidized ilmenite and the activation of the ilmenite during the redox cycles, both the reactivity of pre-oxidized and activated ilmenite was analyzed. The experimental tests were carried out in a thermogravimetric analyzer (TGA), using $H_2$, CO or $CH_4$ as reducing gases, and $O_2$ for the oxidation step. Thus, it was analyzed the reactivity with the main reacting gases when natural gas, syngas or coal are used as fuel in a CLC system. The changing grain size model (CGSM) was used to predict the evolution with time of the solid conversion and to determine the kinetic parameters. In most cases, the reaction was controlled by chemical reaction in the grain boundary. In addition, to predict the behaviour of the oxidation during the first redox cycle of pre-oxidized ilmenite, a mixed resistance between chemical reaction and diffusion in the solid product was needed. The kinetic parameters of both reduction and oxidation reactions of the pre-oxidized and activated ilmenite were established. The reaction order for the main part of the reduction reactions of pre-oxidized and activated ilmenite with $H_2$, CO, $CH_4$ and $O_2$ was $n = 1$, being different ($n = 0.8$) for the reaction of activated ilmenite with CO. Activation energies from 109-165 kJ/mol for pre-oxidized ilmenite and from 65-135 kJ/mol for activated ilmenite were found for the different reactions with $H_2$, CO and $CH_4$. For the oxidation reaction activation energies found were lower, 11 kJ/mol for pre-oxidized and 25 kJ/mol for activated ilmenite.

* Corresponding author: Tel.: +34 976 733977. Fax: +34 976 733318. E-mail: abad@icb.csic.es (A. Abad)

Finally, simplified models of the fuel and air reactors were used to do an assessment of the use of ilmenite as oxygen carrier in a CLC system. The reactor models use the reaction model in the particle and the kinetic parameters obtained in this work. Taking into account for its oxygen transport capacity, the moderated solids inventory and the low cost of the material, ilmenite presents a competitive performance against synthetic oxygen carriers when coal or syngas are used as fuel.

*Keywords:* Combustion; Energy; Fuel; Kinetics; Chemical-Looping Combustion; Ilmenite

## 1. Introduction

Chemical-Looping Combustion (CLC) is one of the most promising technologies to carry out $CO_2$ capture at a low cost (Ekström et al., 2009; IPCC, 2005; Kerr, 2005). CLC is based on the transfer of the oxygen from air to the fuel by means of a solid oxygen carrier. In the most common configuration, the oxygen carrier circulates between two interconnected fluidized beds –the fuel reactor and the air reactor– avoiding direct contact between fuel and air. Figure 1 shows a general scheme of this process. In the fuel reactor the oxygen carrier is reduced through oxidation of the fuel. If the composition of the fuel gas is expressed as $C_nH_mO_l$, the reduction reaction is

$$(2p+q/2-r)\ Me_xO_y + C_pH_qO_r \rightarrow (2p+q/2-r)\ Me_xO_{y-1} + p\ CO_2 + q/2\ H_2O \quad (1)$$

where $Me_xO_y$ denotes a metal oxide and $Me_xO_{y-1}$ its reduced compound. The oxygen carrier reduced in the fuel reactor, $Me_xO_{y-1}$, is transferred to the air reactor where reaction (2) with oxygen from air takes place. Thus the oxygen carrier is regenerated to start a new cycle.

$$2\ Me_xO_{y-1} + O_2 \rightarrow 2\ Me_xO_y \quad (2)$$

In a CLC system, the stream of combustion gases from the fuel reactor contains primarily $CO_2$ and $H_2O$. Water can be easily separated by condensation and a highly concentrated stream of $CO_2$ ready for sequestration is achieved. Thus, the $CO_2$ capture is inherent to this process, as the air does not get mixed with the fuel, and virtually a 100% of $CO_2$ capture can be reached in a CLC system without additional costs or energy penalties for gas separation. Moreover, the net chemical reaction is the same as at usual combustion with the same combustion enthalpy.

The fuel can be a gaseous, liquid or solid compound. On the one hand, natural gas and syngas have been widely proven as gaseous fuels (Lyngfelt, 2010). On the other hand, the in-situ gasification of solid fuels is a relevant option to process them in a CLC system (Leion et al., 2008a). Pyrolysis and gasification of the solid fuel take place in the fuel reactor, and the oxygen carrier, $Me_xO_y$, reacts with the gaseous products, where $H_2$, CO and volatile matter are main components. Against the use of syngas from coal gasification as fuel gas in a CLC system, the direct use of coal in the CLC process has the benefit of avoiding the need of a gasifier and oxygen for coal gasification.

To design a CLC system it is necessary to define the reducing agents of the oxygen carrier. For gaseous fuels, the main reacting gases in the fuel reactor are $CH_4$, CO and $H_2$. When solid fuels are used, the direct reduction of the solid material with carbon also is possible (Siriwardane et al., 2009). However, in a CLC system the reduction by volatiles and the gasification gases, i.e. $H_2$ and CO, should have a higher relevance, and the effect of reduction by carbon should be negligible at temperatures lower than 1300 K (Dey et al., 1993; Donskoi et al., 2003; Sohn and Fruehan, 2005).

### 1.1. The oxygen carrier

Most of the oxygen carriers proposed in the literature are synthetic materials. In general, the oxygen carrier is based on a transition state metal oxide, e.g. CuO, NiO, CoO, $Fe_2O_3$ or $Mn_3O_4$, which is supported on different inert materials, as $Al_2O_3$, $SiO_2$, $TiO_2$ or $ZrO_2$. A selection of oxygen carrier materials for natural gas and syngas combustion has been summarized by Hossain and de Lasa (2008) and Lyngfelt et al. (2008). In addition, there is an increasing interest for the application of CLC regarding the intensive use of coal for energy generation. As a consequence of the ashes present in the solid fuel it is necessary the draining of ashes from the system to avoid its accumulation in the reactors, being predictable a partial loss of the oxygen carrier together the coal ashes. Although synthetic materials –mainly based on Fe, Cu and Ni– have been proposed as oxygen carriers in CLC for solid fuels, e.g. coal, petroleum coke, biomass or solid wastes (Cao et al., 2006; Chuang et al., 2008; Leion et al., 2007; Scott et al., 2006; Shen et al., 2009; Siriwardane et al., 2009; Yang et al., 2007), low cost of the carrier is rather desirable for its use. The use of natural minerals or industrial waste products for this option seems to be very promising (Leion et al., 2009a). These authors analyzed the behaviour of several iron ores, and Fe and Mn industrial products during repeated redox cycles at fluidizing conditions. They concluded ilmenite –a natural mineral mainly

composed of $FeTiO_3$– meet all criteria to be considered as an oxygen carrier for CLC with solid fuels.

Comparing the performance of several natural iron ores and industrial products, ilmenite was ranged among the materials which showed higher reactivity (Leion et al, 2009a and 2009b). The gas conversion showed by ilmenite was even similar to one manufactured $Fe_2O_3/MgAl_2O_4$ selected from previous works because their good performance for CLC applications (Leion et al., 2008a). In addition, the use of ilmenite as oxygen carrier has shown to have high conversion for syngas applications, where CO and $H_2$ are the main components. However, moderate conversion of $CH_4$ for the use of natural gas as fuel was obtained (Leion et al., 2008b). Ilmenite showed high stability in its reactivity after repeated redox cycles. Additionally, ilmenite showed good mechanical stability and good fluidizing properties (Leion et al., 2009a). Defluidization occurred only when the ilmenite particles were in a highly reduced state (Leion et al., 2008b), which is not expected at CLC operation. It should be mentioned that the same ilmenite particles have been used in a 10-kW CLC unit for long periods without difficulties of defluidization (Berguerand and Lyngfelt, 2008a and 2008b).

The effect of successive redox cycles on the ilmenite performance was analyzed in a previous work (Adánez et al., 2010). Ilmenite's reactivity has found to be increasing with the cycle number during first 5-20 cycles, so called the activation period, and after this period its reactivity was maintained roughly constant. The number of cycles of the activation period depended on the reduction conversion reached in every cycle and the reducing gas used. The activation of ilmenite particles is a process relatively fast. Thus, the activation of ilmenite can be done in the CLC system itself, being not necessary the previous activation of ilmenite. Moreover, the fraction of hematite increased at expense of pseudobrookite with the redox cycles. As consequence, the oxygen transport capacity of ilmenite particles decreased with the redox cycles. Moreover, the pre-oxidation of ilmenite particles was considered in order to improve properties, the initial reaction rates and decrease the time for the activation period. Thus, a thermal pre-treatment before feeding ilmenite to the CLC system is appropriate.

### 1.2. Kinetics of reaction for CLC

A key parameter for the design of a CLC system is the solids inventory in the fuel and air reactors as well as the recirculation rate of oxygen carriers between the reactors. Both parameters are linked and depend on the reactivity of the materials and on the oxygen transport capacity of the oxygen carrier (Abad et al., 2007a). The oxygen carrier

must have enough reactivity to fully convert the coal in the fuel reactor, and to be regenerated in the air reactor. Therefore to design a CLC system it is necessary to determine the reactivity under different operating conditions of temperature and gas concentration. It must be considered that the oxygen carrier will be found in different environments during their stage in the fluidized bed reactors. In addition, the modelling of the reactor would be helpful for the design, optimization, and scale-up of the process, in order to obtain high combustion efficiencies in a CLC system. To obtain theoretical results which could be validated against experimental data, the kinetics of reduction and oxidation of the oxygen carrier must be determined.

The kinetics of reaction for the reduction with the main reducing gases present in a CLC system, i.e. $CH_4$, CO and $H_2$, and the oxidation with oxygen have been determined for CuO-, NiO-, $Fe_2O_3$ and $Mn_3O_4$-based oxygen carriers, as it was reviewed by Hossain and de Lasa (2008). The shrinking core model, the changing grain size model and the nucleation model have been widely used to determine the kinetic parameters. However, most of these works give only limited information to apply the kinetics parameters in a mathematical model for the CLC system, because either the effect of the gas concentration or temperature has not been analyzed. Only a limited number of studies have focused on the kinetics of oxygen carriers considering the variation of gas concentration and reactor temperature that could happen in a CLC system, i.e. covering a wide range of gas concentration and temperature representative of the appearing in the air and fuel reactors (Abad et al, 2007a and 2007b; Bohn et al., 2009; Chuang et al., 2009a and 2009b; García-Labiano et al., 2004 and 2006; Ishida et al, 1996; Moghtaderi et al., 2010; Sedor et al., 2008; Zafar et al., 2007a and 2007b). Moreover, less are the studies focused on the kinetics of one certain oxygen carrier with all the reducing gases when natural gas, syngas or coal are used as fuel, mainly $CH_4$, CO and $H_2$ (Abad et al., 2007a; García-Labiano et al., 2004; Moghtaderi et al., 2010). It is necessary to point out that CO and $H_2$ appear as intermediate products during the reaction of $CH_4$ or coal, being necessary to know the reaction kinetic with CO and $H_2$ even if $CH_4$ or coal are used as fuel gas (Abad et al., 2009).

No works about the reaction kinetics of natural minerals for CLC uses –such as ilmenite– were found. Ilmenite is a natural mineral mainly composed of $FeTiO_3$, being the principal source for the production of titanium dioxide, which is widely used in the metallurgy and pigment industries. One process used commonly to obtain titanium dioxide from ilmenite is the high-temperature (1300-1500 K) reduction of iron present

in ilmenite to produce metallic iron and titanium dioxide, which subsequently may be separated by ore-dressing methods. As an alternative, it is possible also to oxidize at temperatures below 1300 K to produce a mixture of titanium dioxide and hematite (Itoh et al., 2006). Then, titanium dioxide is recovered by ore-dressing or aqueous leaching methods. Oxidation of ilmenite to pseudobrookite ($Fe_2TiO_5$) also has been suggested as a pre-treatment before subsequent reduction because it has been found that reduction of ilmenite is enhanced by the pre-oxidation of ilmenite (Park and Ostrovski, 2004; Sun et al., 1993; Zhang and Ostrovski, 2002).

Thus, an intensive work has been done in the past about the reactivity and kinetic determination of the reduction of ilmenite for metallurgical applications using $H_2$ (Bardi et al., 1987; Grey et al., 2007; Sun et al., 1992b and 1993; Vries and Grey, 2006; Zhao and Shadman, 1991), CO (Park and Ostrovski, 2003; Zhao and Shadman, 1990), $CH_4$ (Zhang and Ostrovski, 2001) or carbon (Wang and Yuan, 2006) as reducing agents. Also the oxidation kinetics of ilmenite has been analyzed in the past because of its relevance on some processes of beneficiation of ilmenite to produce rutile (Jabloński and Przepiera, 2001; Rao and Rigoud, 1975; Sun et al, 1992a and 1993).

However, the application of the experience achieved for metallurgical applications, where high reducing potentials are used, can not be directly applied to the reactions involved in the CLC process by several reasons. Firstly, most of the works done about the reduction of ilmenite are focused in the reduction of the iron present in $FeTiO_3$ to metallic iron. However, when ilmenite is used as oxygen carrier, $FeTiO_3$ is the most reduced compound, while pseudobrookite ($Fe_2TiO_5$) is the oxidized form. Moreover, the thermal pre-treatment of ilmenite particles has beneficial effects on its reactivity, thus pre-oxidized ilmenite should be preferred to fresh ilmenite as initial material. Only few works have dealt with the reduction of pre-oxidized ilmenite particles, i.e. the reduction of pseudobrookite (Sun et al., 1992b and 1993). In these works, the kinetic of reaction of pre-oxidized particles was analyzed according to a two-interface kinetic model, where the overall reduction is assumed to follow two steps: reaction (I) the reduction of $Fe^{3+}$ in pseudobrookite to $Fe^{2+}$ in ilmenite; and reaction (II) the reduction of $Fe^{2+}$ to metallic iron. Thus, the reduction reaction occurring in a CLC system corresponds to reaction (I).

Secondly, the analysis of the ilmenite reactivity in the past was limited to the oxidation and reduction of either fresh or pre-oxidized ilmenite particles, as it is necessary for metallurgical applications. On the contrary, in a CLC system the solid particles suffer

from repeated reduction and oxidation cycles, which can affect their chemical and physical properties. Thus, even though the oxidation of ilmenite particles and the reduction step of pre-oxidized ilmenite have been analyzed for metallurgical applications, the reaction kinetics for the oxidation and reduction should be different among unused and activated ilmenite.

### 1.3. Objective

The objective of this work was to analyze the reactivity of pre-oxidized and activated ilmenite particles for CLC applications. The kinetic parameters of the oxidation with oxygen and the reduction with the main reducing gases -as much for gaseous fuels as for solid fuels- existing in a CLC system (CO, $H_2$ and $CH_4$) were established. As ilmenite increases its reactivity with the cycle number, the reactivity of pre-oxidized and activated ilmenite was analyzed. The kinetic parameters obtained will be useful for the design and optimization of a CLC system using ilmenite as oxygen carrier for both gaseous and solids fuels.

## 2. Experimental section

The effect of the main operating variables (type of fuel, gas concentration and temperature) on the oxidation and reduction reaction rates of the selected ilmenite was determined. The experimental tests were carried out in a thermogravimetric analyzer (TGA), using CO, $H_2$ or $CH_4$ as reducing gases, and $O_2$ for the oxidation step. Thus, it was analyzed the reactivity with the main products gases from coal gasification in the fuel reactor, i.e. CO and $H_2$ from coal gasification, and $CH_4$ as a representative gas from coal devolatilization.

### 2.1. Ilmenite

A Norwegian ilmenite was used in this study. The raw material is a concentrate from a natural ore and it has a purity of 94.3%. This material is mainly composed of ilmenite ($FeTiO_3$), rutile ($TiO_2$) and some hematite ($Fe_2O_3$). SEM-EDX analyses revealed a Fe:Ti molar ratio around 1:1. Also minor amounts of oxides and silicates can be found, with $MgSiO_3$ and $MnO_2$ as main compounds. The particle size used for kinetics determination was 150-300 μm. This ilmenite has been showing good reactivity and excellent properties from both TGA and batch fluidized bed testing (Adánez et al., 2010; Leion et al., 2008a, 2008b, 2009a and 2009b). It has also been tested with solid fuel in a 10 kW unit at Chalmers University of Technology (Berguerand and Lyngfelt, 2008a and 2008b).

Pre-oxidized ilmenite and activated particles were used in this work. Pre-oxidized ilmenite was obtained after a thermal treatment of fresh ilmenite at 1223 K in air during 24 hours. During the thermal treatment ilmenite ($FeTiO_3$) was fully oxidized to pseudobrookite ($Fe_2TiO_5$). In a previous work (Adánez et al., 2010), it was found that ilmenite activates through consecutive redox cycles. During activation period the reactivity of ilmenite particles increases and the $Fe_2O_3$ content increases at expense of $Fe_2TiO_5$. After the activation period the reactivity was maintained roughly constant, although the $Fe_2O_3$ content was still increasing. Activated ilmenite used in this work was obtained after 30 redox cycles in a fluidized bed using 25 vol% $CH_4$ + 10 vol% $H_2O$ at 1173 K for the reduction period, guaranteeing the complete activation of the ilmenite particles. The solid conversion reached in the cycles was ≈50%, defined for the reduction reaction from $Fe^{3+}$ to $Fe^{2+}$, i.e. from $Fe_2TiO_5$ and $Fe_2O_3$ to $FeTiO_3$ and FeO, respectively.

Table 1 shows the chemical composition for pre-oxidized and activated ilmenite. The XRD analysis of pre-oxidized and activated particles revealed ferric pseudobrookite ($Fe_2TiO_5$), rutile ($TiO_2$) and some free hematite ($Fe_2O_3$) as major components. It can be seen that the fraction of hematite increases in the activated ilmenite regarding to pre-oxidized particles.

The oxygen transport capacity of ilmenite $R_{o,ilm}$ was calculated as

$$R_{o,ilm} = \frac{m_o - m_r}{m_o} \tag{3}$$

where $m_o$ and $m_r$ are the mass of the most oxidized and reduced form of the oxygen carrier, respectively. In the CLC process, pseudobrookite ($Fe_2TiO_5$) and hematite ($Fe_2O_3$) are reduced to ilmenite ($FeTiO_3$) and magnetite ($Fe_3O_4$), respectively. Rutile is considered to be an inert. Higher reduction prevents the complete conversion of the fuel to $CO_2$ and $H_2O$ because thermodynamic constrictions (Leion et al., 2008b). Thus, $R_{o,ilm}$ was defined as the oxygen transport capacity useful for CLC, and took the values 4.0 wt% for pre-oxidized ilmenite and 3.3 wt% for activated ilmenite. This difference was due to the effect of the ilmenite composition on the mass in the reduced state, $m_r$. The mass corresponding to this reduced state is $m_r$ in equation (3), which increases as the hematite content increases giving a lower value of $R_{o,ilm}$.

SEM pictures of pre-oxidized and activated particles can be seen in Fig. 2. For pre-oxidized ilmenite a granular structure of the solid is observed, which is enhanced during

the activation period, together with a gain in porosity. The porosity of pre-oxidized ilmenite was 1.2 %, whereas for activated ilmenite the porosity value was as high as 12.7 %. From SEM observation, the mean size of the grains was determined to be about 1 μm for pre-oxidized ilmenite and about 2.5 μm for activated ilmenite. More detail about the ilmenite composition and physical properties of ilmenite particles can be found elsewhere (Adánez et al., 2010).

**2.2. Experimental setup**

The kinetic of the reduction and oxidation reactions for the pre-oxidized and activated ilmenite has been carried out through thermogravimetric analysis in a CI thermobalance, see Fig. 3. TGA experiments allowed analyzing the reactivity of the oxygen carriers under well-defined conditions. The reactor consists of two concentric quartz tubes (24 mm i.d. and 10 mm i.d.) placed in an oven. The sample-holder was a wire mesh platinum basket (14 mm diameter and 8 mm height) designed to reduce mass transfer resistance around the solid sample. The temperature and sample weight were continuously collected and recorded in a computer. $N_2$ (2.5 $cm^3$ $s^{-1}$ STP) flowed through the microbalance head to kept the electronic parts free of reactant gas. The reacting gas mixture (~7 $cm^3$ $s^{-1}$ STP) was measured and controlled by electronic mass flow controllers. The reacting gas mixture was introduced at the upper part of the reaction tube. The gas was heated at the desired temperature flowing down through the external annulus of the reactor before contacting with the sample, which was located at the bottom of the reactor. The gas left the reactor through an internal quartz tube after mixing with the gas coming from the head of the balance.

For the reactivity experiments, the ilmenite particles were loaded in the platinum basket. The sample weight used for the experiments was about 50 mg. The oxygen carrier particles were heated up to the desired temperature in an air atmosphere. Once the set temperature was reached, the experiment was started by exposing the oxygen carrier to the desired conditions for the reduction step. In order to avoid the mixing of combustible gas and air, nitrogen was introduced for two minutes between the oxidizing and the reducing period.

The reactivity with the main reacting gases considered being in a CLC system, i.e. $CH_4$, CO and $H_2$ was analyzed. The composition of the gas used to determine the kinetic of the reduction reactions was varied to cover a wide range of gas concentrations (fuel gas, 5-50 vol%; $H_2O$, 20 vol%; $CO_2$, 20 vol%; $O_2$, 5-21 vol%). The temperature was varied from 1073 to 1223 K. For the kinetic determination, the data used corresponded to the

first reduction or oxidation period. Moreover, the same sample of solid particles was not used to obtain the reaction rate at different conditions, but for each experimental condition a new sample of solid particles was used. This procedure was necessary because the reactivity of ilmenite varies with the number of cycles, mainly during the first cycles using pre-oxidized ilmenite.

As much pre-oxidized as activated ilmenite were in its fully oxidized state. To analyze the reactivity of the oxidation reaction it was necessary to reduce the sample first until the particles were composed of $Fe_3O_4$ and $FeTiO_3$, so simulating the behaviour expected in a CLC system. The previous reduction step was carried out at 1173 K in an atmosphere composed of 5 vol% $H_2$ and 40 vol% $H_2O$ ($N_2$ to balance). At these conditions, the reduction of $Fe_2O_3$ was stopped in the $Fe_3O_4$ compound because thermodynamically is unfavourable the subsequent reduction to FeO. After that, ilmenite particles were ready to be oxidized. The oxygen concentration was varied from 5 to 21 vol%, and the reacting temperature was in the range 1073-1223 K. Studies carried out by TGA showed that the oxidation rate was the same independently of the gas previously used for the reduction.

Initially, to establish whether external film mass transfer and/or inter-particle diffusion were affecting the reaction rate, the gas flow rate and the sample weight were varied in the range 6-14 $cm^3\ s^{-1}$ STP and from 20 to 60 mg, respectively. It was observed that the reaction rate was not affected by the amount of sample used or the flow rate, indicating that external and inter-particle diffusion was not of importance. Moreover, several experiments showed that particle sizes in the range 90-500 μm did not affect the reaction rates, excepting for the oxidation of pre-oxidized particles. In this case, the particle size affected to the reactivity in some extension. In the other cases, the internal mass-transfer resistances were not important.

### 2.3. Data evaluation

The reduction of ilmenite components, i.e. pseudobrookite and hematite, by the different reducing gases are given by the following reactions

for reduction with $H_2$

$$Fe_2TiO_5 + TiO_2 + H_2 \rightarrow 2\ FeTiO_3 + H_2O \quad (4)$$

$$3\ Fe_2O_3 + H_2 \rightarrow 2\ Fe_3O_4 + H_2O \quad (5)$$

for reduction with CO

$$Fe_2TiO_5 + TiO_2 + CO \rightarrow 2\ FeTiO_3 + CO_2 \quad (6)$$

$$3\ Fe_2O_3 + CO \rightarrow 2\ Fe_3O_4 + CO_2 \quad (7)$$

for reduction with $CH_4$

$$4\ Fe_2TiO_5 + 4\ TiO_2 + CH_4 \rightarrow 8\ FeTiO_3 + CO_2 + 2\ H_2O \quad (8)$$

$$12\ Fe_2O_3 + CH_4 \rightarrow 8\ Fe_3O_4 + CO_2 + 2\ H_2O \quad (9)$$

For the oxidation reaction, it can be expected that the reaction follows as

$$4\ FeTiO_3 + O_2 \rightarrow 2\ Fe_2TiO_5 + 2\ TiO_2 \quad (10)$$

$$4\ Fe_3O_4 + O_2 \rightarrow 6\ Fe_2O_3 \quad (11)$$

However, the mechanism of oxidation can be some more complex. From thermodynamic calculations (Borowiec and Rosenqvist, 1981; Itoh et al., 2006), the end-product after the oxidation of ilmenite at temperatures higher than 853 K is pseudobrookite ($Fe_2TiO_5$) and rutile ($TiO_2$). However, the end-product experimentally observed when ilmenite is oxidized by air depends on the reacting time and temperature. Rao and Rigaud (1975) found three different oxidation products depending on the temperature of oxidation. Thus, hematite ($Fe_2O_3$) and titanium dioxide ($TiO_2$) were the final products in the temperature range of 773-1023 K; hematite and pseudorutile ($Fe_2Ti_3O_9$) were the final products at 1043-1163 K; and pseudobrookite ($Fe_2TiO_5$) and rutile ($TiO_2$) were identified as oxidation products above 1173 K. Karkhanavala and Momin (1959) and Gupta et al. (1991) found that ilmenite oxidized at temperatures lower than 1123 K produced a mixture of hematite, pseudobrookite and rutile. The metastable compounds $Fe_2O_3 \cdot TiO_2$ and $Fe_2Ti_3O_9$ can appear as intermediate products at temperatures lower than 1273 K (Zhang and Ostrovski, 2002). In short, pseudobrookite was found to be the only end-product when the oxidation was carried out at high temperature (>1123 K) and during long time (>24h), but a mixture of different compounds can be found at lower temperatures or lower oxidation time.

Following the above consideration, the oxidation of ilmenite ($FeTiO_3$) can be considered as:

$$2\ FeTiO_3 + 1/2\ O_2 \rightarrow Fe_2O_3 \cdot 2TiO_2 \rightarrow Fe_2O_3 + 2\ TiO_2 \quad (12)$$

$$3\ FeTiO_3 + 3/4\ O_2 \rightarrow Fe_2Ti_3O_9 + 1/2\ Fe_2O_3 \rightarrow 3/2\ Fe_2TiO_5 + 3/2\ TiO_2 \quad (13)$$

being the end-product a mixture of $Fe_2TiO_5$, $Fe_2O_3$ and $TiO_2$ in a ratio which depends on the reacting time and temperature. Besides, the segregation of $Fe_2O_3$ from the titanium-rich phase also has been reported at 973 K because of the migration of $Fe^{2+}$ and $Fe^{3+}$ ions through the solid lattice towards the grain boundary (Nell, 1999). Once iron is segregated from the titanium-rich phase, the formation of $Fe_2TiO_5$ product is prevented because there is not physical contact between them. Thus, the amount of free $Fe_2O_3$ can be increased after every redox cycle, as it was confirmed from experimental

results in a previous work (Adánez et al., 2010). In addition, the oxidation of the $Fe_3O_4$ coming from the previous reduction of $Fe_2O_3$ also is described by reaction (11).

During the ilmenite reduction, the oxygen transferred to the fuel gas is the sum of the contribution of the reduction of $Fe_2TiO_5$ and $Fe_2O_3$. More complex is the interpretation of the oxygen gained during the oxidation step, as has been above showed, because new hematite appeared. Unfortunately, from the analysis of the thermogravimetric curves it was not possible to separate the contribution in the gaining or losing weight of each one of the reactions (4-13). Therefore, the "Integrated Rate of Reduction" (IRoR) was used, by which the total rate of reduction of a whole particle is used instead of the local rate of reduction (LRoR). The IRoR has been widely used for the analysis of the reduction of iron ores, as it was reviewed by Donskoi et al. (2003). In the IRoR model, the pseudobrookite was considered to be $Fe_2O_3$+$TiO_2$, ilmenite was FeO+$TiO_2$, and magnetite was $Fe_2O_3$+FeO. $TiO_2$ was considered to be an inert material. So, the reduction and oxidation sequence of ilmenite can be summarized and simply expressed as the following two reactions:

$$Fe_2O_3 + H_2 \rightarrow 2\,FeO + H_2O \quad (14)$$

$$Fe_2O_3 + CO \rightarrow 2\,FeO + CO_2 \quad (15)$$

$$4\,Fe_2O_3 + CH_4 \rightarrow 8\,FeO + CO_2 + 2\,H_2O \quad (16)$$

$$4\,FeO + O_2 \rightarrow 2\,Fe_2O_3 \quad (17)$$

where $Fe_2O_3$ includes all the ferric materials, and FeO the ferrous materials, as was used by Sun et al. (1992b). It is worth nothing that magnetite ($Fe_3O_4$) was considered as a mixture of $Fe_2O_3$ and FeO. Therefore, the reduction of hematite to magnetite is assumed to be due to the reduction of 1/3 of the hematite containing iron to FeO, being the remaining 2/3 of iron not reduced.

The conversion level of the oxygen carrier was calculated for the reduction ($X_r$) and oxidation ($X_o$) reactions as

$$X_r = \frac{m_o - m}{R_{o,ilm} m_o} \quad (18)$$

$$X_o = 1 - X_r = \frac{m - m_r}{R_{o,ilm} m_o} \quad (19)$$

The oxygen transport capacity of ilmenite, $R_{o,ilm}$, was 4.0 wt% and 3.3 wt% for pre-oxidized and activated ilmenite respectively, as previously discussed.

## 3. Results

### 3.1. Analysis of the reduction reaction

The reactivity of pre-oxidized and activated ilmenite was investigated using $H_2$, CO or $CH_4$ as reducing gas. To determine the kinetic parameters of the reduction reaction, several experiments at different temperatures (1073, 1123, 1173 and 1223 K) and gas concentrations (5%, 15%, 30%, 50%) were carried out.

#### 3.1.1. Effect of the gas products on the reduction reaction

To analyze the effect of the gas product, i.e. $H_2O$ and $CO_2$, on the reaction rate of the ilmenite, experiments were done with $H_2$ or CO as reacting gases and varying the ratio $H_2O/H_2$ or $CO_2/CO$, respectively. Fig. 4 shows the thermograms obtained for activated ilmenite with 5 vol% $H_2$ and $H_2O$ content from 0 to 30 vol%. Similar curves were obtained for pre-oxidized ilmenite or with 5 vol% CO varying the $CO_2$ content.

When $H_2O$ was not present in the reaction gas mixture the mass loss was about 5% in 200 s. This value is higher than the oxygen transport capacity showed for activated ilmenite, i.e. $R_{o,ilm}$ = 3.3%. The excess in the mass loss was due to the reduction of $Fe_3O_4$ to FeO, or even for longer times, to Fe. In addition, it can be seen two reaction zones. Until a decrease in the initial mass about 3.3% the reaction was fast, but later the reaction rate decreased with time. The mass loss observed during the first step was assigned to the reduction of $Fe_2TiO_5$ and $Fe_2O_3$ to $FeTiO_3$ and $Fe_3O_4$, respectively. In this case, the reaction rate was not affected by the $H_2O$ content because both reductions are allowed by thermodynamic considerations at all the experimental conditions used. However, the subsequent reaction –corresponding to the reduction of $Fe_3O_4$- is clearly affected by the $H_2O$ content: a higher amount of $H_2O$ in the reacting gases leads to a lower reaction rate. This reaction was ceased with $H_2O$ content higher than 20 vol.% when the mass loss was 3.3 wt% because the reduction of $Fe_3O_4$ was avoided due to thermodynamic reasons. The equilibrium constant for the reduction of $Fe_3O_4$ to FeO is 2.1 for $H_2$ and 1.6 for CO at 1173 K (Barin, 1989). This means that the reduction of $Fe_3O_4$ is prevented when $H_2O/H_2 > 2.7$ or $CO_2/CO > 2.1$, as it can be seen in Fig. 4. At these conditions, the final solid products are $FeTiO_3$ and $Fe_3O_4$.

Another consequence of the thermodynamic restrictions for the reduction of $Fe_3O_4$ is that ilmenite should be reduced at maximum to a mixture of $FeTiO_3$ and $Fe_3O_4$ to get complete conversion of gases to $CO_2$ and $H_2O$ in a CLC system. Thus, the corresponding value taking for $R_{o,ilm}$ was 3.3 wt%. Further losses in the mass were not considered to happen in a CLC system, i.e. the oxygen present in $Fe_3O_4$ was not accounted.

The following conversion vs. time curves were calculated from the mass loss showed in the thermograms at different conditions (gas composition and temperature) using equation (18). Conversions higher than 100% –which corresponds to the dotted line– could be obtained in experiments when the mass loss exceeded these values, i.e. for $H_2O/H_2 < 2.7$ or $CO_2/CO < 2.1$. As further reduction of $FeTiO_3$ to $Fe^0$ or $Fe_3O_4$ to wustite (FeO) must be prevented in a CLC system, only the part of the curve up to conversion of 100% was of interest for CLC applications, i.e. the reduction until $FeTiO_3$ and $Fe_3O_4$, which is scarcely affected by the product gas concentration.

### 3.1.2. Effect of fuel type

The study carried out about reactivity showed the different behaviour obtained for the three fuel gases considered in the fuel reactor, i.e. $H_2$, CO and $CH_4$. To compare ilmenite reactivity with these gases, Fig. 5(a) and (b) show the conversion vs. time curves for the different reducing gases for pre-oxidized and activated ilmenite, respectively. Observe that the time scales are different in these Figures.

Although ilmenite presents initially a rather low reactivity, there is an important reactivity increase after the activation period. For the different reducing gases, pre-oxidized and activated ilmenite react faster with $H_2$ than with CO and $CH_4$, reaching a conversion value of 80% in 35 s. Pre-oxidized ilmenite reacts faster with CO than with $CH_4$, unlike activated ilmenite. For $H_2$ and CO the reactivity rises around 5 times after the activation, while for $CH_4$ this increase is about 15 times. The reactivity increase observed for all these fuel gases can be explained through the structural changes undergoing the solid during consecutives redox cycles (Adánez et al., 2010).

### 3.1.3. Effect of gas concentration

To determine the effect of the gas concentration on the kinetics of the reduction reaction, several experiments at 1173 K and gas concentrations (5, 15, 30 and 50%) were carried out. As example, Fig. 6 shows plots of the effect of $H_2$ concentration on the conversion-time curves. Similar behaviour was observed for CO and $CH_4$. As expected, an increase in the fuel gas concentration produces an increase on the reaction rate.

### 3.1.4. Effect of temperature

The effect of temperature on the reaction rate of ilmenite was later investigated. Fig. 7 shows the conversion vs. time curves for the reduction with CO of pre-oxidized and activated ilmenite. Similar curves were obtained for $H_2$ and $CH_4$. In all cases, the reaction rate is quite affected by the temperature. An increase of temperature produces an increase on the reduction rate.

### 3.2. Analysis of the oxidation reaction

The CLC system is composed of two interconnected fluidized bed reactors. The reduced oxygen carrier from the fuel reactor is regenerated in the air reactor. Therefore, the regeneration of the oxygen carrier with air should be also analyzed. The oxidation reactivity of pre-oxidized and activated ilmenite was investigated. As the solid samples were completely oxidized, before the oxidation step they were fully reduced until $FeTiO_3$ and $Fe_3O_4$ using 5 vol% $H_2$ and 40 vol% $H_2O$. To determine the kinetic parameters of the oxidation reaction several experiments at different temperatures (1073, 1123, 1173 and 1223 K) and oxygen concentrations (5%, 10%, 15%, 21%) were carried out.

Fig. 5 shows the conversion vs. time curves obtained for pre-oxidized and activated ilmenite, together those obtained for the reduction with $H_2$, CO and $CH_4$. The reactivity of the oxidation reaction is higher than those for the reduction with $H_2$, CO, and $CH_4$, except for the oxidation of pre-oxidized ilmenite for solid conversions higher than ≈0.25. After this value, the reaction rate sharply decreased for pre-oxidized ilmenite. Nevertheless, the complete oxidation of pre-oxidized particles was obtained after a long enough oxidizing period. To analyze the reason for this strong decrease of the reactivity at a conversion ≈0.25, different samples of pre-oxidized particles were fully reduced and later oxidized for different times. Thus, samples of ilmenite particles with different conversion of oxidation were obtained. SEM images of these particles are shown in Fig. 8. It can be seen that the fully reduced particle exhibits a granular and porous structure. This structure was still maintained when the particle was partially oxidized to $X_o$ = 0.2, but it can be seen some decrease in the porosity development. However, the porosity collapsed when particles were further oxidized at $X_o$ = 0.5 and 0.8. This fact suggests that the reaction mechanism probably changes from a chemical reaction control to a diffusional control in the particle due to the loss of porosity inside the particle as oxidation proceeds. This fact agrees to the results showed by other authors. Rao and Rigaud (1975) observed a quick decrease on the oxidation reaction rate at conversion varying from 0.3 to 0.75, which depended on the particle size. They suggested that this decrease was due to the formation of a thick adherent film around the particle. Sun et al. (1992a) determined that oxidation of ilmenite was mainly controlled by the intrinsic kinetic and diffusional effects in the product layer, being the diffusion more important as the oxidation proceeds.

After the activation period, it was found a considerable increase in the reaction rate, which is more pronounced for solid conversions higher than ≈0.25, see Fig. 5. On the contrary than for pre-oxidized ilmenite, for activated ilmenite the initial porosity is high enough to be conserved after the oxidation step, as can be seen in Table 1. Thus, the oxidation reaction of activated ilmenite is relatively fast and mainly controlled by the chemical reaction in the solid surface. A conversion value as high as 80% is obtained in 15 s.

#### 3.2.1. Effect of oxygen concentration

Several experiments were carried out at 1173 K with different $O_2$ concentration (5, 10, 15 and 21%). Fig. 9 shows the conversion-time curves obtained for pre-oxidized and activated ilmenite. It can be observed that the reaction rate increases as the $O_2$ concentration increases when the reaction rate was controlled by the chemical reaction. However, the $O_2$ concentration scarcely affects the reaction rate when the reaction was controlled by diffusion in the particle, i.e. when the reaction rate was slow for pre-oxidized ilmenite.

#### 3.2.2. Effect of temperature

Several experiments were carried out at different temperatures from 1073 to 1223 K with a constant oxygen concentration of 21 vol %, and following the procedure described in the experimental section. Fig. 10 shows the conversion vs. time curves obtained for pre-oxidized and activated ilmenite. Contrary to the effect showed for the reduction reaction, the oxidation rate scarcely increased when the temperature was increased, mainly when the reaction was controlled by the chemical reaction. Some higher effect of the temperature was observed when the reaction was controlled by diffusion in the particle, i.e. the oxidation of pre-oxidized particles for $X_o > 0.25$.

### 3.3. Determination of the kinetic parameters

By using a particle reaction model, the kinetic parameters of the different reactions can be determined for the oxygen carrier. Most of reaction models used for the oxidation of ilmenite (Jabloński and Przepiera, 2001; Rao and Rigaud, 1975; Sun et al., 1992a) and the reduction of pre-oxidized ilmenite (Sun et al., 1992b) were based on a mixed control of chemical reaction at the grain boundary and diffusion in the particle. Other reaction models, as nucleation models, have been refused in the past to describe the oxidation reaction of ilmenite (Rao and Rigaud, 1975).

The requirements that must fulfil a model are to be a representation as near as possible to the real process and that can be coupled without many difficulties with the fluidized

bed reactor model. Several SEM images showed a granular structure inside the ilmenite particles (see Fig. 2). Moreover, previous studies showed that the particle size did not affect the reaction rates of ilmenite. Taking into account for these considerations and the results showed by other authors, the grain model with uniform reaction in the particle with changing grain size model in the grains, controlled by chemical reaction, was used to determine the kinetic parameters.

The model assumes that the particle consists of a number of nonporous spherical grains of uniform initial radius, $r_g$. The reaction proceeds in the grain following the changing grain size model. Considering that the reaction is controlled by the reaction in the grain which corresponds to negligible resistances to gas film mass transfer and diffusion inside the particle, the equations that describe this model are the following:

$$\frac{t}{\tau_{chr}} = 1-(1-X_i)^{1/3} \qquad \tau_{chr} = \frac{\rho_m r_g}{\bar{b} k_s C_g^n} \tag{20}$$

In addition, to predict the behaviour of the oxidation of pre-oxidized ilmenite a mixed resistance between chemical reaction and diffusion in the solid product was needed, as previously has been discussed. In this case, it was assumed that the reaction rate was controlled by chemical reaction in the grain up to a determined conversion value, $X_{chr}$, which will be determined from the conversion-time curves. During this period, the porosity of particles decreases because the volume of the solid products ($Fe_2TiO_5$+$TiO_2$ and $Fe_2O_3$) is higher than those for the solid reactants ($FeTiO_3$ and $Fe_3O_4$). This chemically controlled step proceeds until the porosity collapses. From this point, it was assumed that the oxidation proceeds following a shrinking core model in the particle, and it is controlled by the diffusion in the solid. Furthermore, it was found that the oxygen concentration do not affect the oxidation rate when the reaction is controlled by diffusion through the product layer. This fact was already showed by Rao and Rigaud (1975), suggesting that iron ions are mobile through the solid lattice, which agrees with the iron segregation observed during the activation process. The equations that describe this oxidation step are the following

$$\frac{t}{\tau_{dif}} = 3\left[1-(1-X_0')^{2/3} + \frac{1-Z+(1-Z)(1-X_0')^{2/3}}{Z-1}\right] \qquad \tau_{dif} = \frac{\rho_m r_p^2}{6\,\bar{\bar{b}}\,D_e} \tag{21}$$

where $Z$ is the expansion ratio between the solid product and solid reactive:

$$Z = \frac{V_{m,prod}}{V_{m,reac}} \tag{22}$$

and $X_0^{'}$ is a modified conversion that takes into account that the diffusional control starts at the conversion $X_{chr}$, and it is calculated as

$$X_o^{'} = \frac{X_o - X_{chr}}{1 - X_{chr}} \tag{23}$$

being $X_0^{'} = 0$ at $X_o = X_{chr}$, and $X_0^{'} = 1$ at $X_o = 1$.

The time necessary to reach any conversion for values higher than $X_{chr}$ is given by

$$t = t_{dif} + t_{chr}\big|_{X_{chr}} \tag{24}$$

$t_{chr}\big|_{X_{chr}}$ is the time at which $X_{chr}$ is reached and it is calculated from eq. (20).

As it has been discussed above, from the conversion vs. time curves it was not possible to differentiate the reduction of $Fe_2TiO_5$ from that of $Fe_2O_3$. Thus, a global kinetic rate constant was calculated for the sum of both reactions, i.e. the reduction of $Fe^{3+}$ to $Fe^{2+}$, as it was expressed by eqs. (14-16). Similarly, a global kinetic rate constant was obtained for the oxidation reaction of $Fe^{2+}$ to $Fe^{3+}$, see eq. (17). In this line, an average coefficient $\bar{b}$ was used in eqs. (20) and (21) as a function of ilmenite composition, which is shown in Table 2.

This kinetic model was used to determine the kinetic parameters for the reduction of pre-oxidized and activated ilmenite with $H_2$, CO and $CH_4$, and the oxidation with $O_2$. The reaction order, $n$, with respect to each reacting gas ($H_2$, CO, $CH_4$ or $O_2$) was obtained from the calculus of $\tau_{chr}$ by fitting the experimental curves conversion-time to the model equation. Thereby, equation (20) can be expressed as follows:

$$\ln\left(\frac{\rho_m\, r_g}{\bar{b}\,\tau_{chr}}\right) = \ln\,(k_s) + n\,\ln\left(C_g\right) \tag{25}$$

From a plot of $\ln(\rho_m r_g/b\tau_{chr})$ vs. $\ln(C_g)$ the values of the reaction order, $n$, can be obtained from the slope of the figure, and the $\ln(k_s)$ at the reaction temperature. Fig. 11 shows this plot for the each reacting gas. The calculated reaction order for each reaction is shown in Table 2.

From the experiments carried out at different temperatures, values for the chemical reaction kinetic constant, $k_s$, as a function of the temperature were obtained. The dependence on the temperature of the kinetic constant was assumed to be Arrhenius type, as follows:

$$k_s = k_{s0} e^{-E_{chr}/R_g T} \tag{26}$$

Fig. 12 shows the Arrhenius plot of the $k_s$ values as a function of $1/T$. The values of the kinetic parameters finally obtained for pre-oxidized and activated ilmenite are given in Table 2.

For the oxidation of pre-oxidized ilmenite, the diffusion in the product layer of the particle was also considered. By fitting the conversion curves obtained at different temperatures, the values of the effective diffusivity in the product layer, $D_e$, at each temperature were obtained. Fig. 12 shows the Arrhenius's plot for the dependence of $D_e$ with the temperature, and the values of the pre-exponential factor and the activation energy finally obtained are given in Table 2.

The theoretical curves calculated using the reaction model with the kinetic parameters showed in Table 2 predicted adequately the experimental results in all range of operating conditions studied for both pre-oxidized and activated ilmenite. As example, some conversion-time curves predicted by the reaction model are shown in Figs. (6-7) and (9-10).

For the reduction reactions, values for activation energies ranged from 109 to 165 kJ/mol for pre-oxidized ilmenite, and lower values, from 65 to 136 kJ/mol were obtained for activated ilmenite. These values are higher than those showed for other iron-based oxygen carriers (Son and Kim, 2006; Abad et al., 2007a and 2007b; Moghtaderi et al., 2010), except for that calculated by Bohn et al. (2009), who referred an activation energy of 75 kJ/mol for the reduction with CO. In addition, the values of the activation energy are in the range of that obtained by Sun et al. (1992b) for different pre-oxidized materials at 1073 K, in which some hematite was found. Lower values of the activation energy were found for the oxidation of pre-oxidized and activated ilmenite (11.8 and 25.5 kJ/mol, respectively), but a higher value was found for the effective diffusivity for pre-oxidized ilmenite (77 kJ/mol). The activation energy for diffusion in the solids during the oxidation reaction was mainly found in the range 46-180 kJ/mol (Rao and Rigaud, 1975; Sun et al., 1993) when the reaction was controlled by lattice diffusion. The lower limit of this range was found for the oxidation when there are a complete segregation among hematite and rutile, whereas the higher limit was found for complete oxidation to pseudobrookite. In this work it was found a value of the activation energy between them, which can be related to a partial segregation of hematite from the titanium rich phase in every redox cycle. A lower value of the activation energy of 31 kJ/mol was found by Jabloński and Przepiera (2001) when the

chemical reaction was controlling the reaction, in line to the results obtained in this work.

## 4. Discussion

A key parameter for the design of a CLC system is the solids inventory in the fuel– and air–reactors as well as the recirculation rate of oxygen–carriers between the reactors. Both parameters are linked and depend on the reactivity of the materials and on the oxygen transport capacity of the oxygen–carrier. In this section the use of the kinetic parameters determined in this work for design purposes is discussed.

### 4.1. Assessment of the use of ilmenite as oxygen carrier

The important parameters in the design of a CLC system are the recirculation rate of particles and the solids inventory. Both the oxygen transport capacity and the reduction and oxidation reactivity of solids determine the solids inventory in the fuel and air reactors to reach full conversion of fuel gas. A simplified model has been used to get an initial estimation of the solids inventory (Abad et al., 2007a). Thus, the calculated solids inventory facilitates the comparison of the feasibility of different oxygen carriers in an adequate way. The simplified model considers perfect mixing of solids, no restriction for the gas-solid contact, and the solid reaction following the shrinking core model. Considering the mass balance to the reactor, the mass of solids in the fuel and air reactors per $MW_{th}$ of fuel, $m_{OC}$, can be calculated for gaseous fuels as (Abad et al., 2007a)

$$m_{OC} = \eta_c \frac{2dM_O}{\Delta H_c^0} \frac{3}{\Phi R_{o,ilm} \left( \left. \frac{dX_i}{dt} \right|_{X_i=0} \right)_{\text{av}}} = \eta_c \frac{2dM_O}{\Delta H_c^0} \frac{3}{\Phi \left( \left| \left. \frac{d\omega}{dt} \right|_{X_i=0} \right| \right)_{\text{av}}} \tag{27}$$

and for solid fuels, e.g. coal, as (Adánez et al., 2010)

$$m_{OC} = \eta_c \frac{10^3 m_O}{\text{LHV}} \frac{3}{\Phi R_{o,ilm} \left( \left. \frac{dX_i}{dt} \right|_{X_i=0} \right)_{\text{av}}} = \eta_c \frac{10^3 m_O}{\text{LHV}} \frac{3}{\Phi \left( \left| \left. \frac{d\omega}{dt} \right|_{X_i=0} \right| \right)_{\text{av}}} \tag{28}$$

being $m_O$ the mass of oxygen required per kg of solid fuel to fully convert the solid fuel to $CO_2$ and $H_2O$, as for the case of the conventional combustion with air. LHV is the lower heating value of the solid fuel. In this work a typical composition for coal of 70% carbon, 5% hydrogen and 10% oxygen has been assumed, corresponding to a value of $m_O$ = 2.2 kg O/kg coal. The LHV was assumed to be 25000 kJ/kg.

Often the rate of oxygen transference is expressed as a mass based conversion rate, d$\omega$/d$t$, where $\omega$ is the mass based conversion defined as

$$\omega = \frac{m}{m_o} = 1 + R_{o,ilm}\left(X_o - 1\right) = 1 - R_{o,ilm}X_r \tag{29}$$

The mass based conversion rate can be calculated as

$$\frac{d\omega}{dt} = R_{o,ilm}\left(\frac{dX_i}{dt}\right) \tag{30}$$

The average reactivities, $\left(\left.\frac{dX_i}{dt}\right|_{X_i=0}\right)_{\text{av}}$ and $\left(\left|\left.\frac{d\omega}{dt}\right|_{X_i=0}\right|\right)_{\text{av}}$, are obtained at the average gas concentration in the reactor and at the conversion of ilmenite $X_i = 0$. For gaseous fuels, the average concentration can be obtained from the following equation

$$\overline{C_g}^{\,n} = \frac{\Delta X_g C_{g0}^n}{\int_{X_{g,in}}^{X_{g,out}} \left[\frac{1+\varepsilon_g X_g}{1-X_g}\right]^n \mathrm{d}X_g} \tag{31}$$

where $\varepsilon_g$ considers the gas expansion as a consequence of the reaction, and it was calculated as

$$\varepsilon_g = \frac{V_{g,X_g=1} - V_{g,X_g=0}}{V_{g,X_g=0}} \tag{32}$$

The value of $\varepsilon_g$ was 2 for the reduction reaction with $CH_4$, 0 for the use of $H_2$ and CO, and -0.21 for the oxidation reaction. Table 3 shows the average concentration considering a gas conversion of $X_{g,out}$ = 99.9% in the fuel reactor, and an air excess of 20 % in the air reactor. For solid fuels, an initial estimation of the solids inventory was calculated only considering $H_2$ and CO proceeding from coal gasification. $H_2$ and CO concentration values can be as low as 2%, as found during CLC continuous operation (Berguerand and Lyngfelt, 2008a and 2008b). Considering that the reactivity of a mixture of $H_2$ and CO is similar to the reactivity for $H_2$ (Abad et al., 2007b), the average reactivity in eq. (28) was calculated for 5% $H_2$, as the sum of $H_2$ and CO concentrations (Adánez et al., 2010).

The parameter $\Phi$ is the characteristic reactivity in the reactor, and it can be easily obtained from Fig. 7 in the work done by Abad et al. (2007a) as a function of the variation of the solids conversion in the reactor, $\Delta X_i$, and the conversion of solids at the reactor inlet. Nevertheless, assuming spherical grains in the kinetic model the value of

characteristic reactivity, Φ, is limited between 3 and 0. The minimum solids inventory in every reactor is obtained considering that Φ = 3, which is the case for $X_{i,in} = 0$ and $\Delta X_i \approx 0$. This condition has been chosen to calculate the solids inventory and it could be reached when there were not limitations for solids circulation between fuel reactor and air reactor. The solids inventories so obtained for pre-oxidized and activated ilmenite are shown in Table 3.

The solids inventory in the air reactor can be also obtained from eqs (27) and (28) for gaseous and solid fuels, respectively. In this case, the average reactivity, i.e. $\left(\left.\frac{dX_i}{dt}\right|_{X_i=0}\right)_{av}$ or $\left(\left|\left.\frac{d\omega}{dt}\right|_{X_i=0}\right|\right)_{av}$, should be the corresponding to the oxidation reaction. As the oxygen demanded by each fuel ($CH_4$, $H_2$, CO or coal) is different per $MW_{th}$ of fuel, the solids inventory per $MW_{th}$ in the air reactor is also different for every fuel gas, even if the oxidation reactivity is the same in all cases. Therefore, a solids inventory in the air reactor can be calculated for each fuel gas, as it is shown in Table 3.

Higher solids inventories were found for pre-oxidized ilmenite than for activated ilmenite because the increase of the reactivity during the activation period. Also lower values of the solids inventory are found for the air reactor than for the fuel reactor because of the higher ilmenite reactivity for the oxidation reaction with respect to the reduction reactions. In the same way, higher solids inventories are required for the use of methane as fuel gas than for the syngas components, i.e. $H_2$ and CO. The solids inventory in the fuel reactor is highly dependent on the reactor temperature because the considerable increase of the reactivity with the temperature. However, minor differences in the solids inventory of the air reactor with the temperature were found because the low activation energy of the oxidation reaction, see Table 2.

The numbers showed in Table 3 can be compared to the solids inventory calculated for several synthethic oxygen carriers (Abad et al., 2007a; Zafar et al.,2007a and 2007b). Activation is expected to occur quickly in the CLC system and it can be considered that most of particles in the CLC system are activated. Thus, only the minimum solids inventory for activated particles will be used for comparison purposes with other oxygen carriers. The solids inventories calculated for the air reactor (30-52 kg/$MW_{th}$) are in the range of those calculated for other Ni-, Cu-, Mn- and Fe-based oxygen carriers, which were in the range 10-60 kg/$MW_{th}$. On the contrary, the calculated solids inventories in the fuel reactor for ilmenite were usually higher than the obtained for

others oxygen carriers. For ilmenite the solids inventories were in the range 42-66 kg/$MW_{th}$ for $H_2$, 105-189 kg/$MW_{th}$ for CO and 167-461 kg/$MW_{th}$ for $CH_4$. For a highly reactive synthethic Fe-based oxygen carrier the solids inventory obtained for $H_2$ and CO were 12 kg/$MW_{th}$ and 29 kg/$MW_{th}$, respectively whereas that the solids inventory for $CH_4$ was 950 kg/$MW_{th}$. Nevertheless, lower solids inventories were calculated for methane using other oxygen carriers, e.g. in the range 10-20 kg/$MW_{th}$ for Ni-based oxygen carriers, 52 kg/$MW_{th}$ for a Cu-based oxygen carrier or 85 kg/$MW_{th}$ for a Mn-based oxygen carrier (Abad et al., 2007a; Zafar et al., 2007a and 2007b).

Regarding the values obtained for the solids inventory and comparing these values with those calculated for synthetic oxygen carriers with proven suitability in a CLC process, the assessment of the use of ilmenite as oxygen carrier can be done. Thus, the use of ilmenite for the combustion of methane is not adequate, but there could be interesting the use of ilmenite for syngas combustion. Also, the solids inventory needed for ilmenite takes also acceptable values for coal combustion and the use of ilmenite for coal it is highly recommended because ilmenite is harmless for the environment and a considerably cheaper material than a synthetic material.

### 4.2. Application of the kinetic data to a reactor model

To predict satisfactorily the experimental results of a CLC plant with the mathematical model, it is necessary to know the actual reactivity of the oxygen carrier in the air and fuel reactors, which should be an average reactivity of all particles inside the reactors. For this purpose, it is necessary to consider how the reactivity of a particle changes during successive redox cycles, and the life-time of every particle in a CLC system until they are elutriated or drained together the coal ashes. Every particle in a CLC has a different lifetime. For example, the number of cycles and the reacting time in each reactor has not to be the same for all particles existing in a CLC system. Thus, the reactivity of every particle would be different.

In a previous work (Adánez et al., 2010) it was found that pre-oxidized ilmenite particles increase their reactivity –here defined as the variation of conversion with time ($dX_i/dt$)– with the number of cycles. Ilmenite conversion $X_i$ of the reduction or oxidation reaction was obtained using eqs. (18) or (19) and considering that free $Fe_2O_3$ and $Fe_2TiO_5$ in ilmenite are reduced up to $Fe_3O_4$ and $FeTiO_3$, respectively. However, the oxygen transport capacity, $R_{o,ilm}$, decreased with the redox cycles because the amount of hematite in the particles increased. From this complex situation, it seems that to know the average reactivity of particles which had different degree of activation –as it is the

case in a CLC system– could be a hard task. That is, the reactivity of newly introduced particles, i.e. pre-oxidized, and particles with different degree of activation should be determined, and then to calculate an average reactivity of the particles in the air and fuel reactors.

To solve this problem and for preliminary estimations, it was assumed that the fraction of non-activated particles in the CLC system is low compared to the activated ones and it can be considered that most of particles in the CLC system are activated. This assumption can be realistic if the activation process was shorter than the lifetime of the particles in the CLC system. This can be the case because the activation of ilmenite particles is a fast process, which happens in a few redox cycles. Moreover, it is necessary to consider that the rate of oxygen transference remains constant after the activation period (Adánez et al., 2010). Thus, the mass based conversion rate, $d\omega/dt$, is maintained constant, and the same value can be obtained from two activated particles with different oxygen transport capacity, i.e.

$$\frac{d\omega}{dt} = R_{o,1}\left(\frac{dX_i}{dt}\right)_1 = R_{o,2}\left(\frac{dX_i}{dt}\right)_2 \quad (33)$$

The reactivity $(dX_i/dt)_1$ of activated particles with an oxygen transport capacity $R_{o,1}$ = 3.3 wt% can be determined from the kinetics parameters obtained in this work. Thus, the reactivity $(dX_i/dt)_2$ of any other particles with an oxygen transport capacity $R_{o,2}$ can be easily determined from eq. (33). Similarly, the average reactivity, $\left(\overline{\frac{dX_i}{dt}}\right)_2$, of a mixture of activated particles with an average oxygen transport capacity $\overline{R}_{o,2}$ can be calculated using the kinetic parameters obtained in this work for activated ilmenite.

As an example, Figure 13 shows the solids inventory in the fuel reactor as a function of the oxygen transport capacity for activated ilmenite and using coal as fuel. As it was shown in a previous work (Abad et al., 2007a), the solids inventory depends on the solids circulation flow-rate, $\dot{m}_{OC}$. Thus, the solids inventory calculated for different values of $\dot{m}_{OC}$ are shown in Fig. 13. It can be seen that the solids inventory decreases as the solids circulation flow-rate increases or the oxygen transport capacity increases. Both parameters, $\dot{m}_{OC}$ and $R_{o,ilm}$, are linked to the variation of solids conversion in the reactor, $\Delta X_i$, by eq. (34) for gaseous fuels and eq. (35) for solids fuels, which is the parameter affecting the solids inventory through the parameter Φ, see eqs. (27) and (28).

$$\Delta X_i = \frac{2dM_O}{R_{o,ilm}\Delta H_c^0}\frac{1}{\dot{m}_{OC}} \tag{34}$$

$$\Delta X_i = \frac{10^3 m_O}{R_{o,ilm}\mathrm{LHV}}\frac{1}{\dot{m}_{OC}} \tag{35}$$

Therefore, as $\dot{m}_{OC}$ or $R_{o,ilm}$ increases, $\Delta X_i$ decreases. Thus, as $\Delta X_i$ decreases the residence time of particles in the reactor should be lower, and the solids inventory decreases. Here, it is useful to remember that the rate of oxygen transference is maintained constant for activated particles with different values of $R_{o,ilm}$, as it was stated in eq. (33). At this condition, the parameter affecting the solids inventory is $\Delta X_i$, i.e. the same solids inventory value will be obtained for a constant value of $\Delta X_i$ corresponding to the same value for the product of $\dot{m}_{OC}$ and $R_{o,ilm}$. In Fig. 13 some reference lines corresponding to various values of $\Delta X_i$ are plotted.

Also it can be observed in Fig. 13 that the effect of the oxygen transport capacity on the solids inventory is less noticeable as the solids circulation rate increases, i.e. when $\Delta X_i$ decreases. This fact is an effect of considering perfect mixing of solids in the reactor. When $\Delta X_i \rightarrow 0$, the fraction of reacting oxygen is much lower than the total available oxygen in particles. Thus, the total available oxygen in the particles, i.e. the oxygen transport capacity, has low relevance on the average reactivity of particles in the reactor and hence in the solids inventory. At the condition $\Delta X_i \rightarrow 0$ the minimum solids inventory is reached, as it was showed in Table 3.

Under these considerations, the kinetic parameters determined in this work can be introduced in a mathematical model describing the reactors of a CLC system when gaseous or solids fuels are used. In a future work, the mathematical model of the CLC system will be used to simulate and optimize the process for industrial operation under different operating conditions.

## 5. Conclusions

The reactivities of the reduction and oxidation reactions for pre-oxidized and activated ilmenite were determined by thermogravimetric analysis using methane, hydrogen, carbon monoxide or oxygen as reacting gases. The activated ilmenite exhibited high reactivity in both reduction and oxidation reactions, with times for complete conversion at 1223 K lower than 120 s using 15% of $H_2$, CO or $CH_4$, and 30 s using 21% of $O_2$.

The kinetic parameters of the reduction reaction with $H_2$, CO or $CH_4$ and the oxidation by oxygen of pre-oxidized and activated particles were obtained. The grain model with uniform reaction in the particle and reaction in the grains following a changing grain size model with chemical reaction control in the grains was used to determine the kinetic parameters. In addition, to predict the behaviour of the oxidation of pre-oxidized ilmenite, a mixed resistance between chemical reaction and diffusion in the solid product was needed.

The reaction order in the main part of the reactions of pre-oxidized and activated ilmenite with $H_2$, CO, $CH_4$ and $O_2$ was $n = 1$, being different ($n = 0.8$) for the reaction of activated ilmenite with CO. Activation energies from 109-165 kJ/mol for pre-oxidized ilmenite and from 65-135 kJ/mol for activated ilmenite were found for the different reactions with $CH_4$, CO and $H_2$. For the oxidation reaction activation energies found were lower: 11 kJ/mol for pre-oxidized and 25 kJ/mol for activated ilmenite.

The activation process has a beneficial and strong influence on the solids inventory needed in both the air and fuel reactor. An analysis of the performance of ilmenite depending on the activation degree has been done. From results showed in this work, it can be concluded that ilmenite presents a competitive performance for its use in CLC against synthetic oxygen carriers when it is taken into account for the oxygen transport capacity, the moderated solids inventory and the low cost of the material. This last issue can be determinant for the selection of an oxygen carrier for solid fuels combustion in a CLC system.

**Notation**

$\bar{b}$ = average stoichiometric coefficient for reaction of solid with reacting gas

$d$ = stoichiometric factor in the fuel combustion reaction with oxygen, mol $O_2$ per mol of fuel

$C_g$ = reacting gas concentration, mol $m^{-3}$

$C_{g0}$ = gas concentration at the reactor inlet, mol $m^{-3}$

$\overline{C}_g$ = average gas concentration in the reactor, mol $m^{-3}$

$D_e$ = effective diffusivity in the product layer, mol $m^{-2}$ $s^{-1}$

$D_{e0}$ = pre-exponential factor for effective diffusivity, mol $m^{-2}$ $s^{-1}$

$E_j$ = activation energy of the reacting mechanism j, kJ $mol^{-1}$

$k_s$= chemical kinetic constant, $mol^{1-n}$ $m^{3n-2}$ $s^{-1}$

$k_{s0}$ = pre-exponential factor for chemical kinetic constant, $mol^{1-n}$ $m^{3n-2}$ $s^{-1}$

$m$ = instantaneous mass of the oxygen carrier, kg

$m_r$ = mass of the reduced form of the oxygen carrier, kg

$m_o$ = mass of the oxidized form of the oxygen carrier, kg

$m_O$ = mass of oxygen required per kg of solid fuel to full convert the solid fuel, kg oxygen/kg coal

$m_{OC}$ = solids inventory, kg per $MW_{th}$

$\dot{m}_{OC}$ = solids circulation rate per $MW_{th}$ of fuel, kg $s^{-1}$ per $MW_{th}$

$M_O$ = molecular weight of oxygen, = 16 g $mol^{-1}$

$n$ = reaction order

$r_g$ = grain radius, m

$r_p$ = particle radius, m

$R_g$ = ideal gas constant, = 8.314 J $mol^{-1}$ $K^{-1}$

$R_{0,ilm}$ = oxygen transport capacity of ilmenite

$t$ = time, s

$t_j$ = reacting time while the mechanism j controlling the reaction is fulfilled, s

$T$ = temperature, K

$V_{g,X_g=0}$ = volume of the gas mixture at $X_g$ = 0, $m^3$

$V_{g,X_g=1}$ = volume of the gas mixture at $X_g$ = 1, $m^3$

$V_{m,prod}$ = molar volume of reacting product, $m^3$ $mol^{-1}$

$V_{m,reac}$ = molar volume of reacting solid, $m^3$ $mol^{-1}$

$X_g$ = gas conversion

$X_i$ = conversion of solids of the reaction i

$X_{chr}$ = particle conversion until chemical reaction control is fulfilled

$X_0^{'}$ = modified conversion, defined by equation (23)

$Z$ = expansion ratio between the solid product and solid reactive

*Greek letters*

$\Delta H_c^0$ = standard combustion heat of the gas fuel, kJ mol$^{-1}$

$\Delta X_g$ = variation of the gas conversion in the reactor

$\Delta X_i$ = variation of the solid conversion in the reactor for the reaction i

$\varepsilon_g$ = coefficient of expansion of the gas mixture

$\Phi$ = characteristic reactivity in the reactor

$\rho_m$= molar density, mol/m$^3$

$\tau_j$ = time for complete conversion by controlling the mechanism j, s

$\omega$ = mass based conversion

*Subscripts*

av = average condition

chr = control by chemical reaction at the solid surface

dif = control by diffusion through the product layer around the particle

in = inlet

o = oxidation reaction

out =outlet

r = reduction reaction

*Abbreviations*

LHV = lower heating value of the solid fuel, kJ kg$^{-1}$

Submitted, accepted and published by
Chemical Engineering Science 66 (2011) 689-702

**Acknowledgments**

This work was partially supported by the European Commission, under the RFCS program (ECLAIR Project, Contract RFCP-CT-2008-0008) and from Alstom Power Boilers. A. Cuadrat thanks CSIC for the JAE Pre fellowship.

## References

Abad, A., Adánez, J., García-Labiano, F., de Diego, L.F., Gayán, P., Celaya, J., 2007a. Mapping of the range of operational conditions for Cu-, Fe-, and Ni-based oxygen carriers in chemical-looping combustion. Chemical Engineering Science 62, 533-549.

Abad, A., García-Labiano, F., de Diego, L.F., Gayán, P., Adánez, J., 2007b. Reduction Kinetics of Cu-, Ni-, and Fe-Based Oxygen Carriers Using Syngas ($CO + H_2$) for Chemical-Looping Combustion. Energy & Fuels 21, 1843-1853.

Abad, A., Adánez, J., García-Labiano, F., de Diego, L.F., Gayán, P., 2009. Modeling of the Chemical-Looping Combustion of Methane using a Cu-based Oxygen Carrier. Energy Procedia 1, 391-398.

Adánez, J., Cuadrat, A., Abad, A., Gayán, P., de Diego, L.F., García-Labiano, F., 2010. Ilmenite Activation during Consecutive Redox Cycles in Chemical-Looping Combustion. Energy & Fuel 24, 1402-1413.

Bardi, G., Gozzi, D., Stranges, S., 1987. High temperature reduction kinetics of ilmenite by hydrogen. Materials Chemistry and Physics 17, 325-341.

Barin, I., 1989. Thermochemical Data of Pure Substances, VCH Publishers, Cambridge.

Berguerand, N., Lyngfelt, A., 2008a. Design and operation of a 10 kWth chemical-looping combustor for solid fuels – Testing with South African coal. Fuel 87, 2713-2726.

Berguerand, N., Lyngfelt, A., 2008b. The use of petroleum coke as fuel in a 10 kWth chemical-looping combustor. Int. J. Greenhouse Gas Control 2, 169-179.

Bohn, C.D., Cleeton, J.P., Müller, C.M., Scott, S.A., Dennis, J.S., 2009. Mesuring the kinetics of the reduction of iron oxide with carbon monoxide in a fluidized bed. Proceedings of the 20$^{th}$ International Conference on Fluidized Bed Combustion, Xian (China), p 555–561.

Borowiec, K., Rosenqvist, T., 1981. Phase Relations and Oxidation Studies in the System Fe-$Fe_2O_3$-$TiO_2$ at 700-1100 ºC. Scandinavian Journal of Metallurgy 10, 217-224.

Cao, Y., Casenas, B., Pan, W.-P., 2006. Investigation of Chemical Looping Combustion by Solid Fuels. 2. Redox Reaction Kinetics and Product Characterization with Coal, Biomass, and Solid Waste as Solid Fuels and CuO as an Oxygen Carrier. Energy & Fuels 20, 1845-1854.

Chuang, S.Y., Dennis, J.S., Hayhurst, A.N. Scott, S.A., 2008. Development and performance of Cu-based oxygen carriers for chemical-looping combustion. Combustion and Flame 154, 109-121.

Chuang, S.Y., Dennis, J.S., Hayhurst, A.N. Scott, S.A., 2009a. Kinetics of the chemical looping oxidation of CO by a co-precipitated mixture of CuO and $Al_2O_3$. Proceedings of the Combustion Institute 32, 2633–2640.

Chuang, S.Y., Dennis, J.S., Hayhurst, A.N., Scott, S.A., 2009b. Kinetics of oxidation of a reduced form of the Cu-based oxygen–carrier for use in Chemical–Looping Combustion. Proceedings of the 20th International Conference on Fluidized Bed Combustion, Xian (China), p 512–518.

Dey, S.K., Jana, B., Basumallick, A., 1993. Kinetics and Reduction Characteristics of Hematite-noncoking Coal Mixed Pellets under Nitrogen Gas Atmosphere. ISIJ Int. 33(7), 735-739.

Donskoi, E., McElwain, D.L.S., Wibberley, L.J., 2003. Estimation and Modeling of Parameters for Direct Reduction in Iron Ore/Coal Composites: Part II. Kinetic Parameters. Met. Mat. Trans. B 34B, 255-266.

Ekström1, C., Schwendig, F., Biede, O., Franco, F., Haupt, G., de Koeijer, G., Papapavlou, C., Røkke, P.E., 2009. Techno-Economic Evaluations and Benchmarking of Pre-combustion $CO_2$ Capture and Oxy-fuel Processes Developed in the European ENCAP Project. Energy Procedia 1, 4233-4240.

García-Labiano, F., de Diego, L.F., Adánez, J., Abad, A., Gayán, P., 2004. Reduction and Oxidation Kinetics of a Copper-Based Oxygen Carrier Prepared by Impregnation for Chemical-Looping Combustion. Ind. Eng. Chem. Res. 43, 8168-8177.

García-Labiano, F., Adánez, J., de Diego, L.F., Gayán, P., Abad, A., 2006. Effect of Pressure on the Behavior of Copper-, Iron-, and Nickel-Based Oxygen Carriers for Chemical-Looping Combustion. Energy & Fuels 20, 26-33.

Grey, I., McDonald, K., Fisher-White, M., de Vries, M., 2007. Hydrogen reduction of peroxidised ilmenite in fluidised bed and packed bed reactors. Mineral Processing and Extractive Metallurgy 116(4), 209-216.

Gupta, S.K., Rajakumar, V., Grievenson, P., 1991. Phase transformations during heating of ilmenite concentrates. Metall. Mater. Trans. B 22B(5), 711-716.

Hossain, M.M., de Lasa, H.I., 2008. Chemical-looping combustion (CLC) for inherent $CO_2$ separations—a review. Chem. Eng. Sci. 63, 4433-4451.

IPCC special report on carbon dioxide capture and storage. 2005. (available at http://ipcc.ch). Chapter 3. Capture.

Ishida, M., Jin, H., Okamoto, T., 1996. A Fundamental Study of a New Kind of Medium Material for Chemical-Looping Combustion. Energy & Fuels 10, 958-963.

Itoh, S., Sato, S., Ono, J., Okada, H., Nagasaka, T., 2006. Feasibility Study of the New Rutile Extraction Process from Natural Ilmenite Ore Based on the Oxidation Reaction. Metallurgical and Materials Transactions B 37B, 979-985.

Jabloński, M., Przepiera, A., 2001. Estimation of kinetic parameters of thermal oxidation of ilmenite. J. Thermal Anal. and Calorimetry 66, 617-622.

Karkhanavala, M.D., Momin, A.C., 1959. The alteration of ilmenite. Econ.Geol. 54, 1095-1102.

Kerr, H.R., 2005. Capture and separation technologies gaps and priority research needs. In: Thomas, D., Benson, S. (Eds.), Carbon Dioxide Capture for Storage in Deep Geologic Formations—Results from the $CO_2$ Capture Project, vol. 1. Elsevier Ltd., Oxford, UK. (Chapter 38).

Leion, H., Mattisson, T., Lyngfelt, A., 2007. The use of petroleum coke as fuel in chemical-looping combustion. Fuel 86, 1947-1958.

Leion, H., Mattisson, T., Lyngfelt, A., 2008a. Solid fuels in chemical-looping combustion. Int. J. Greenhouse Gas Control 2, 180-193.

Leion, H., Lyngfelt, A., Johansson, M., Jerndal, E., Mattisson, T., 2008b. The use of ilmenite as an oxygen carrier in chemical-looping combustion. Chem. Eng. Res. Des. 86, 1017-1026.

Leion, H., Mattisson, T., Lyngfelt, A., 2009a. Use of Ores and Industrial Products As Oxygen Carriers in Chemical-Looping Combustion. Energy & Fuels 23, 2307-2315.

Leion, H., Jerndal, E., Steenari, B.-M., Hermansson, S., Israelsson, M., Jansson, E., Johnsson, M., Thunberg, R., Vadenbo, A., Mattisson, T., Lyngfelt, A., 2009b. Solid fuels in chemical-looping combustion using oxide scale and unprocessed iron ore as oxygen carriers. Fuel 88, 1945-1954.

Lyngfelt, A., Johansson, M., Mattisson, T., 2008. Chemical-Looping Combustion – Status of Development. Proceedings of the 9th International Conference on Circulating Fluidized Beds (CFB-9), Hamburg, Germany.

Lyngfelt, A., 2010. Oxygen carriers for chemical-looping combustion - Operational experience. Proceedings of the 1st International Conference on Chemical Looping, IFP–Lyon (France).

Moghtaderi, B., Song, H., Doroodchi, E., Wall, T., 2010. Reactivity analysis of mixed metal oxides. Proceedings of the 1st International Conference on Chemical Looping, IFP–Lyon (France).

Nell, J., 1999. An overview of the phase-chemistry involved in the production of high-titanium slag from ilmenite feedstock. Heavy Minerals, 137-145.

Park, E., Ostrovski, O., 2003. Reduction of Titania-Ferrous Ore by Carbon Monoxide. ISIJ Int. 43(9), 1316-1325.

Park, E., Ostrovski, O., 2004. Effect of Preoxidation of Titania-Ferrous Ore on the Ore Structure and Reduction Behavior. ISIJ Int. 44(1), 74-81.

Rao, D.B., Rigaud, M., 1975. Kinetics of the oxidation of ilmenite. Oxidation of Metals 9(1), 99-116.

Scott, S.A., Dennis, J.S., Hayhurst, A.N., Brown, T., 2006. In Situ Gasification of a Solid Fuel and $CO_2$ Separation using Chemical Looping. AIChE J. 52, 3325-3328.

Sedor, K.E., Hossain, M.M., de Lasa, H.I., 2008. Reduction Kinetics of a Fluidizable Nickel-Alumina Oxygen Carrier for Chemical-Looping Combustion. The Canadian J. of Chem. Eng. 86, 323-334.

Shen, L., Wu, J., Xiao, J., Song, Q., Xiao, R., 2009. Chemical-Looping Combustion of Biomass in a 10 kWth Reactor with Iron Oxide as an Oxygen Carrier. Energy&Fuels 23, 2498-2505.

Siriwardane, R., Tian, H., Richards, G., Simonyi, T., Poston, J., 2009. Chemical-Looping Combustion of Coal with Metal Oxide Oxygen Carriers. Energy & Fuels, doi: 10.1021/ef9001605.

Sohn, I., Fruehan, R.J., 2005. The Reduction of Iron Oxides by Volatiles in a Rotary Hearth Furnace Process: Part I. The Role and Kinetics of Valetile Reduction. Met. Mat. Trans. B 36B, 605-612.

Son, S.R., Kim, S.D., 2006. Chemical–Looping Combustion with NiO and $Fe_2O_3$ in a thermobalance and circulating fluidized bed reactor with double loops. Industrial & Engineering Chemistry Research 45, 2689-2696.

Sun, K., Ishii, M., Takahashi, R., Yagi, J.-I., 1992a. Oxidation Kinetics of Cement-bonded Natural Ilmenite Pellets. ISIJ Int. 32(4), 489-495.

Sun, K., Ishii, M., Takahashi, R., Yagi, J.-I., 1992b. Reduction Kinetics of Cement-bonded Natural Ilmenite Pellets with Hydrogen. ISIJ Int. 32(4), 496-504.

Sun, K., Takahashi, R., Yagi, J.-I., 1993. Kinetics of the Oxidation and Reduction of Synthetic Ilmenite. ISIJ Int. 33(5), 523-528.

Vries, M.L., Grey, I.E., 2006. Influence of Pressure on the Kinetics of Synthetic Ilmenite Reduction in Hydrogen. Met. Mat. Trans. B 37B, 199-208.

Wang, Y., Yuan, Z., 2006. Reductive kinetics of the reaction between a natural ilmenite and carbon. Int. J. Miner. Process. 81, 133-140.

Yang, J.-b., Cai, N.-s., Li, Z.-s., 2007. Reduction of Iron Oxide as an Oxygen Carrier by Coal Pyrolysis and Steam Char Gasification Intermediate Products. Energy & Fuels 21, 3360-3368.

Zafar, Q., Abad, A., Mattisson, T., Gevert, B., 2007a. Reaction Kinetics of Freeze-Granulated NiO/$MgAl_2O_4$ Oxygen Carrier Particles for Chemical-Looping Combustion. Energy & Fuels 21, 610-618.

Zafar, Q., Abad, A., Mattisson, T., Gevert, B., Strand, M., 2007b. Reduction and oxidation kinetics of $Mn_3O_4$/Mg-$ZrO_2$ oxygen carrier particles for chemical-looping combustion. Chem. Eng. Sci. 62, 6556-6567.

Zhang, G., Ostrovski, O., 2001. Reduction of ilmenite concentrates by methane containing gas, Part II: Effects of preoxidation and sintering. Canadian Metallurgical Quarterly 40(4), 489-497.

Zhang, G., Ostrovski, O., 2002. Effect of preoxidation and sintering on properties of ilmenite concentrates. Int. J. Miner. Process. 64, 201-218.

Zhao, Y., Shadman, F., 1990. Kinetics and Mechanism of Ilmenite Reduction with Carbon Monoxide. AIChE J. 36, 1433-1438.

Zhao, Y., Shadman, F., 1991. Reduction of Ilmenite with Hydrogen. Ind. Eng. Chem. Res. 30, 2080-2087.

**Captions of Figures**

Fig. 1. General scheme of a Chemical-Looping Combustion system.

Fig. 2. SEM images of (a) calcined and (b) activated ilmenite particles.

Fig. 3. CI thermobalance layout.

Fig. 4. Thermograms obtained during the reduction of activated ilmenite using different $H_2O/H_2$ ratios. $H_2$ = 5%. $N_2$ to balance. $T$ = 1173 K.

Fig. 5. Conversion vs. time curves during reduction period using $H_2$, CO or $CH_4$ as reducing agent (continuous lines). Also the oxidation by air is showed for the reduced ilmenite (broken lines). (a) pre-oxidized ilmenite; (b) activated ilmenite. Experimental conditions: $T$ = 1173 K; reducing gas mixtures: 15% $H_2$ + 20% $H_2O$ or 15% CO + 20% $CO_2$ or 15% $CH_4$ + 20% $H_2O$. Nitrogen to balance.

Fig. 6. Effect of $H_2$ concentration on the reduction reaction for (a) pre-oxidized and (b) activated ilmenite. $T$ = 1173 K. $H_2$ concentration: ° 5 vol%; ▵ 15 vol%; ◇ 30 vol%; ▫ 50 vol%. 20 vol% $H_2O$; $N_2$ to balance. Continuous line: model predictions.

Fig. 7. Effect of CO concentration on the reduction reaction for (a) pre-oxidized and (b) activated ilmenite. Temperature: ° 1073 K; ▵ 1123 K; ◇ 1173 K; ▫ 1223 K. 15 vol% CO; 20 vol% $CO_2$; $N_2$ to balance. Continuous line: model predictions.

Fig. 8. SEM images of pre-oxidized ilmenite particles after one reduction step (a) and at different conversion of the following oxidation: (b) $X_o$ = 0.2; (c) $X_o$ = 0.5; (d) $X_o$ = 0.8.

Fig. 9. Effect of $O_2$ concentration on the oxidation reaction for (a) pre-oxidized and (b) activated ilmenite. $T$ = 1173 K. $O_2$ concentration: ° 5 vol%; ▵ 10 vol%; ◇ 15 vol%; ▫ 21 vol%. $N_2$ to balance. Continuous line: model predictions.

Fig. 10. Effect of temperature on the oxidation reaction for (a) pre-oxidized and (b) activated ilmenite. Temperature: ° 1073 K; ▵ 1123 K; ◇ 1173 K; ▫ 1223 K. 21 vol% $O_2$; $N_2$ to balance. Continuous line: model predictions.

Fig. 11. Plot to obtain the reaction order with respect to $H_2$, CO and $CH_4$, and $O_2$ for (a) pre-oxidized and (b) activated ilmenite. $T$ = 1173 K. ° $H_2$; ▵ CO; ◇ $CH_4$; ▫ $O_2$.

Fig. 12. Arrhenius plot for the kinetic constant $k_s$ for the reaction of $H_2$, CO, $CH_4$ and $O_2$ and the effective diffusivity, $D_e$, for the oxidation with (a) pre-oxidized and (b) activated ilmenite. $k_s$: ° $H_2$; ▵ CO; ◇ $CH_4$; ▫ $O_2$. $D_s$: ■ $O_2$

Fig. 13. Solids inventory for activated ilmenite (kg of solids per $MW_{th}$ of fuel) as a function of the oxygen transport capacity for several solids circulation flow-rate, $\dot{m}_{OC}$ (kg $s^{-1}$ per $MW_{th}$). $T$ = 1223 K; $X_{i,in}$ = 0.5-$\Delta X_i$/2.

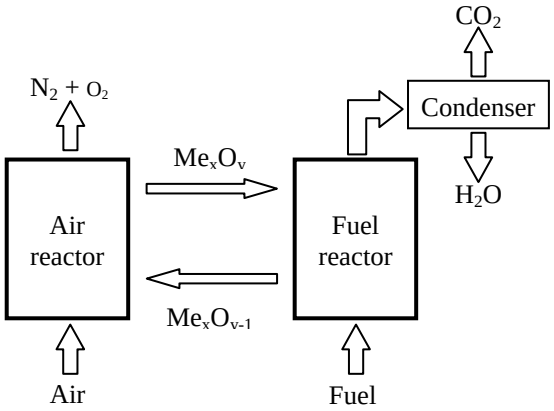


Fig. 1. General scheme of a Chemical-Looping Combustion system.

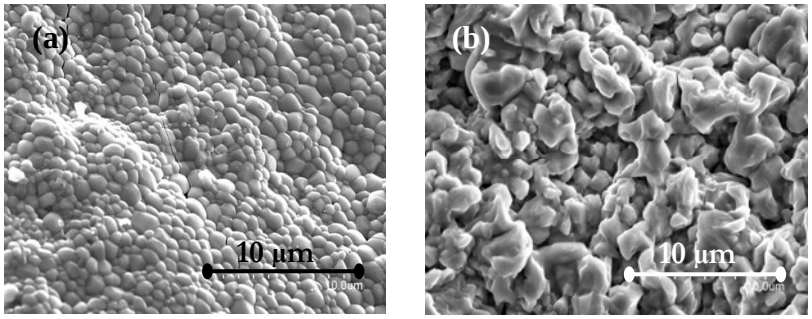


Fig. 2. SEM images of (a) calcined and (b) activated ilmenite particles.

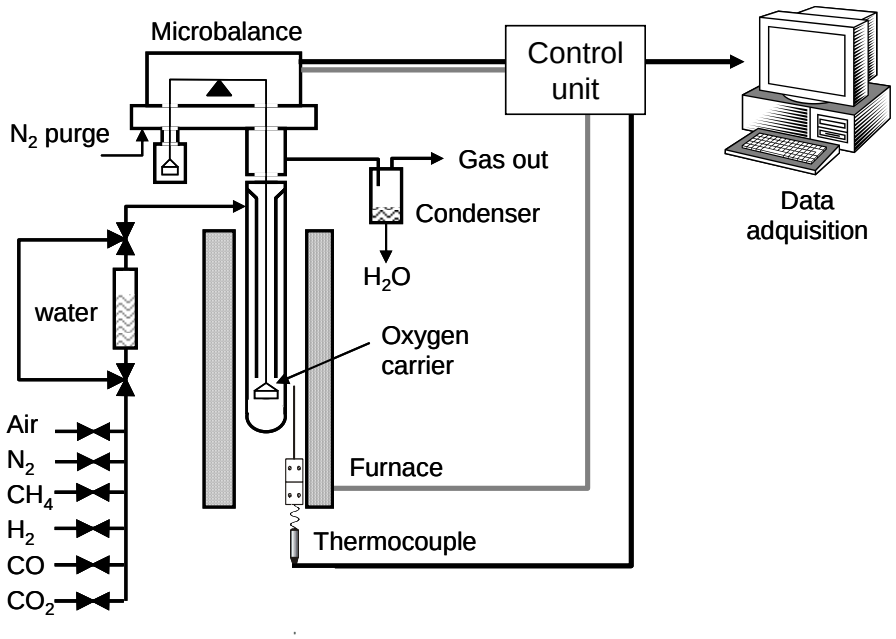


Fig. 3. CI thermobalance layout.

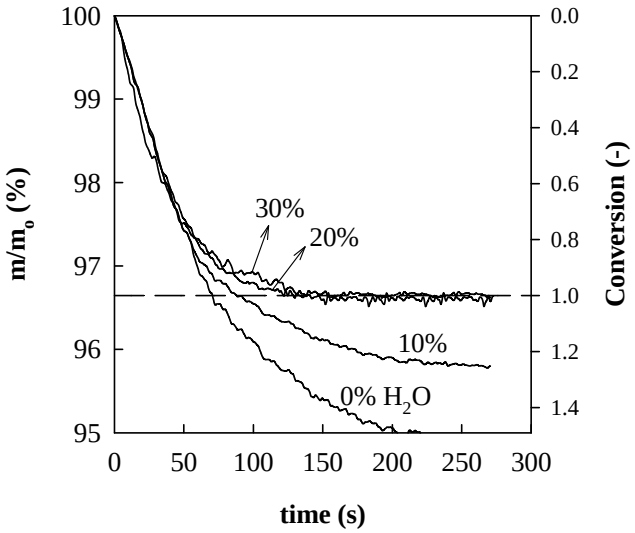


Fig. 4. Thermograms obtained during the reduction of activated ilmenite using different $H_2O/H_2$ ratios. $H_2$ = 5%. $N_2$ to balance. $T$ = 1173 K.

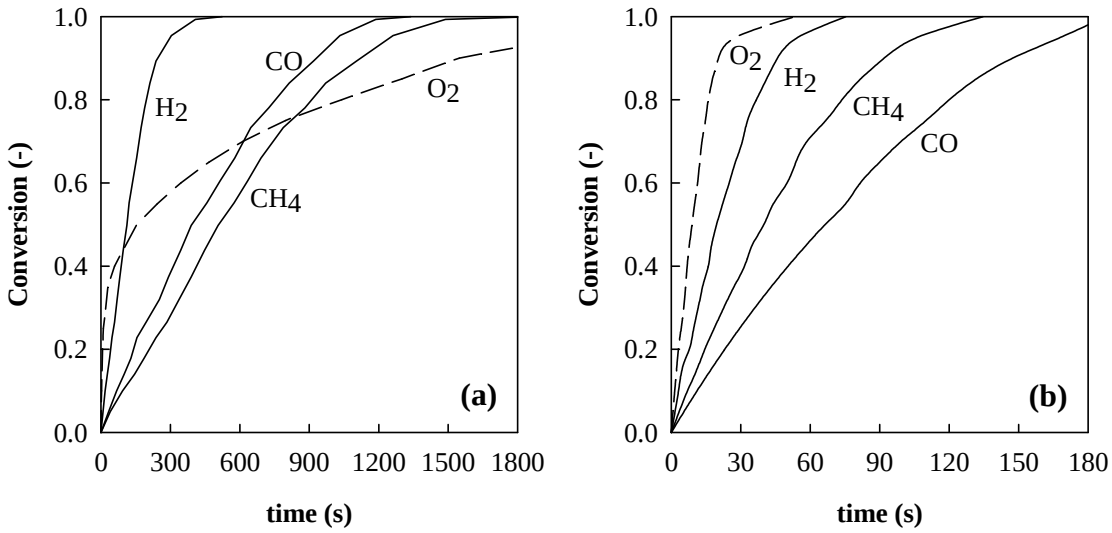


Fig. 5. Conversion vs. time curves during reduction period using $H_2$, CO or $CH_4$ as reducing agent (continuous lines). Also the oxidation by air is showed for the reduced ilmenite (broken lines). (a) pre-oxidized ilmenite; (b) activated ilmenite. Experimental conditions: $T$ = 1173 K; reducing gas mixtures: 15% $H_2$ + 20% $H_2O$ or 15% CO + 20% $CO_2$ or 15% $CH_4$ + 20% $H_2O$. Nitrogen to balance.

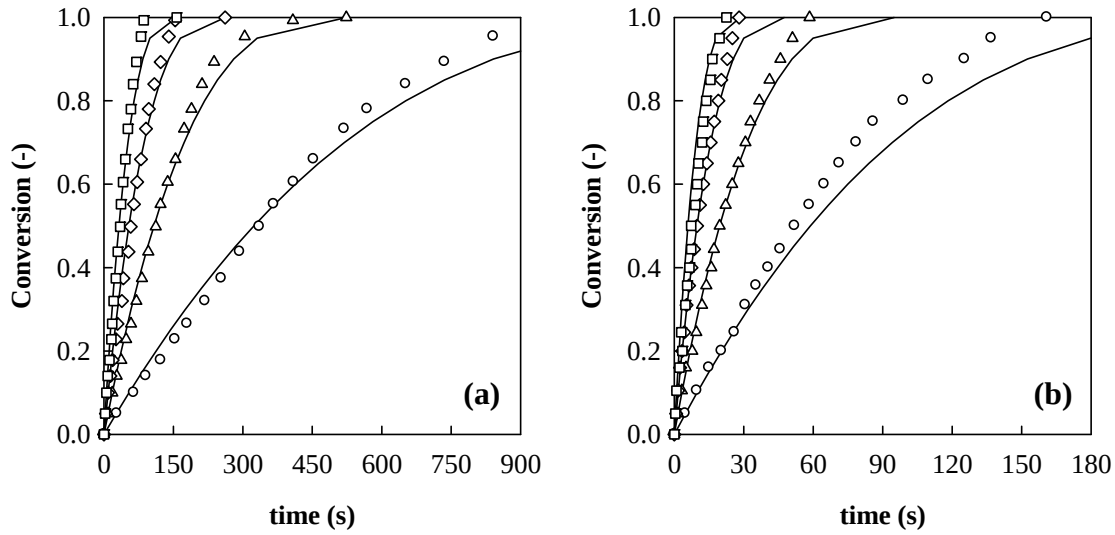


Fig. 6. Effect of $H_2$ concentration on the reduction reaction for (a) pre-oxidized and (b) activated ilmenite. $T$ = 1173 K. $H_2$ concentration: ○ 5 vol%; △ 15 vol%; ◇ 30 vol%; □ 50 vol%. 20 vol% $H_2O$; $N_2$ to balance. Continuous line: model predictions.

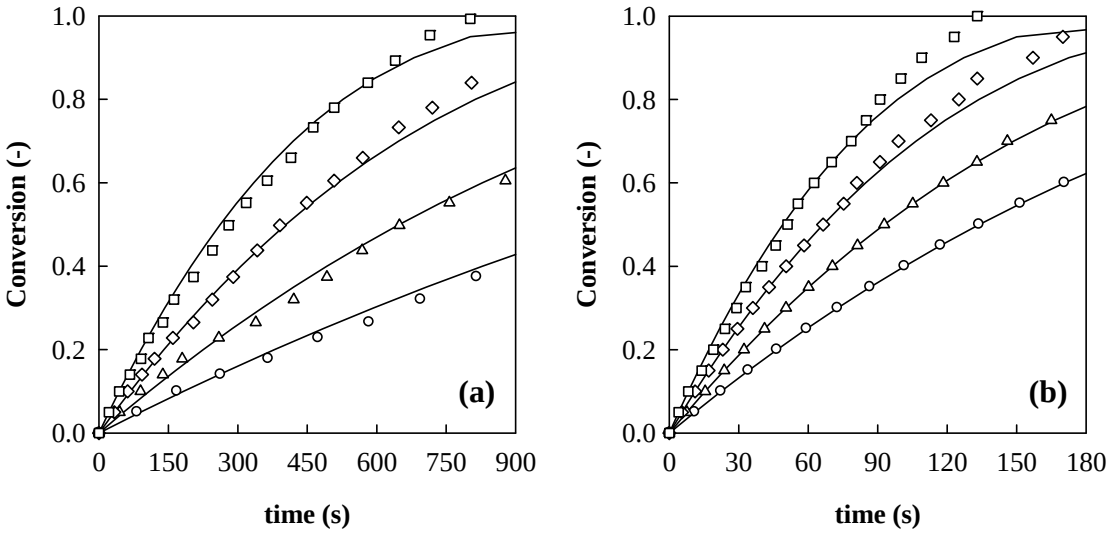


Fig. 7. Effect of CO concentration on the reduction reaction for (a) pre-oxidized and (b) activated ilmenite. Temperature: ° 1073 K; △ 1123 K; ◇ 1173 K; ▫ 1223 K. 15 vol% CO; 20 vol% $CO_2$; $N_2$ to balance. Continuous line: model predictions.

Reaction Kinetics of Ilmenite for Chemical-Looping Combustion.
Alberto Abad, Juan Adánez, Ana Cuadrat, Francisco García-Labiano, Pilar Gayán, and Luis F. de Diego.

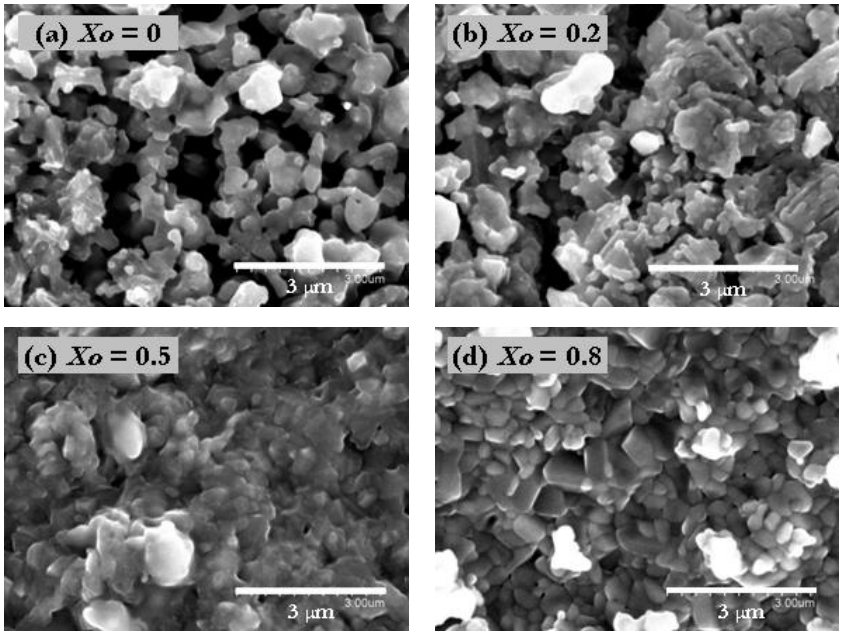


Fig. 8. SEM images of pre-oxidized ilmenite particles after one reduction step (a) and at different conversion of the following oxidation: (b) $X_o$ = 0.2; (c) $X_o$ = 0.5; (d) $X_o$ = 0.8.

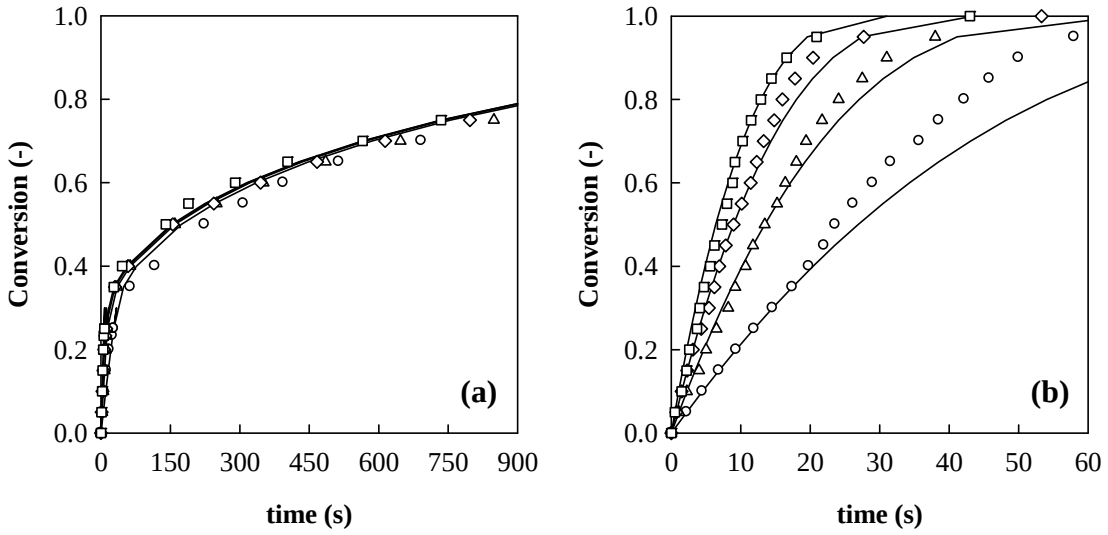


Fig. 9. Effect of $O_2$ concentration on the oxidation reaction for (a) pre-oxidized and (b) activated ilmenite. $T$ = 1173 K. $O_2$ concentration: ° 5 vol%; △ 10 vol%; ◇ 15 vol%; □ 21 vol%. $N_2$ to balance. Continuous line: model predictions.

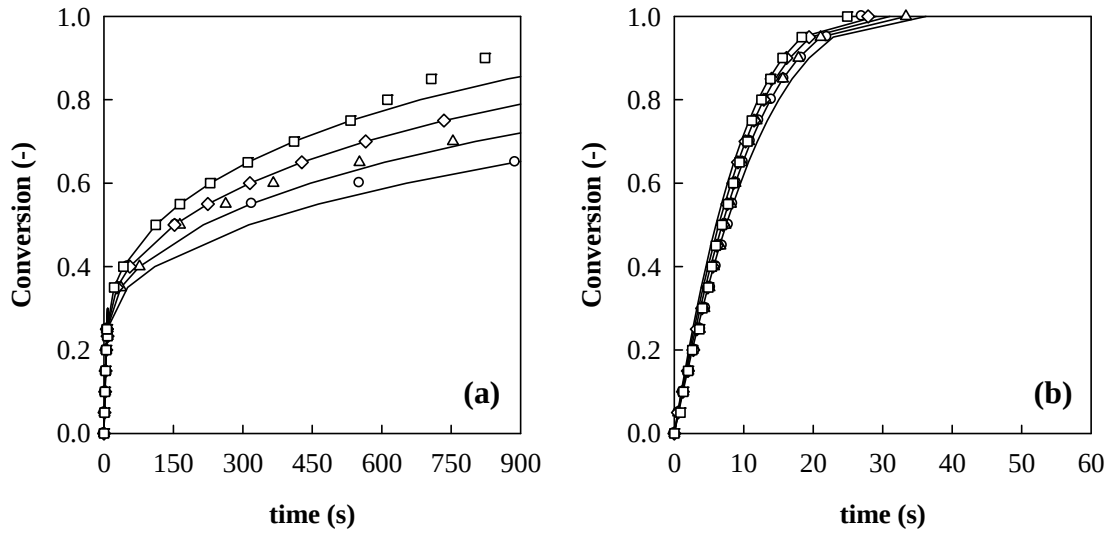


Fig. 10. Effect of temperature on the oxidation reaction for (a) pre-oxidized and (b) activated ilmenite. Temperature: ° 1073 K; △ 1123 K; ◇ 1173 K; ▫ 1223 K. 21 vol% $O_2$; $N_2$ to balance. Continuous line: model predictions.

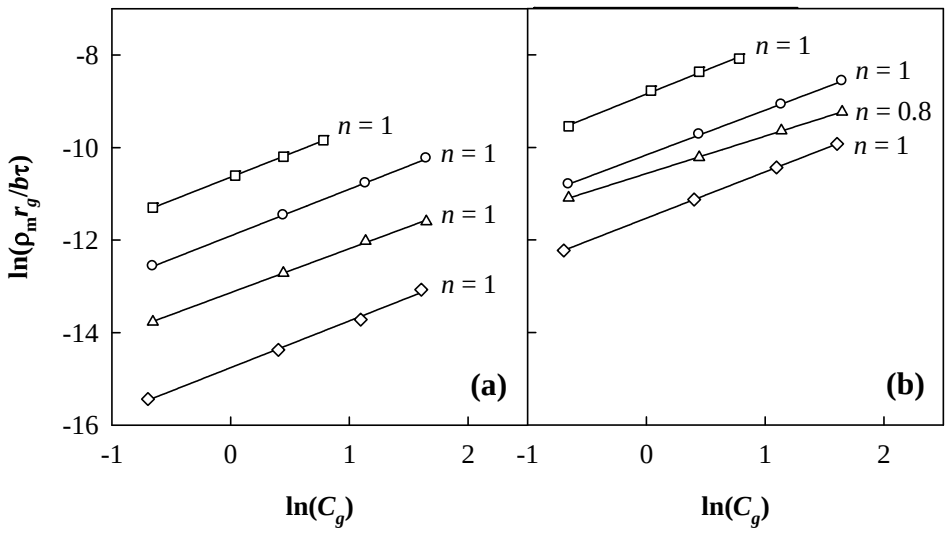


Fig. 11. Plot to obtain the reaction order with respect to $H_2$, CO and $CH_4$, and $O_2$ for (a) pre-oxidized and (b) activated ilmenite. $T$ = 1173 K. ° $H_2$; ▵ CO; ◇ $CH_4$; ▫ $O_2$.

Reaction Kinetics of Ilmenite for Chemical-Looping Combustion.
Alberto Abad, Juan Adánez, Ana Cuadrat, Francisco García-Labiano, Pilar Gayán, and Luis F. de Diego.

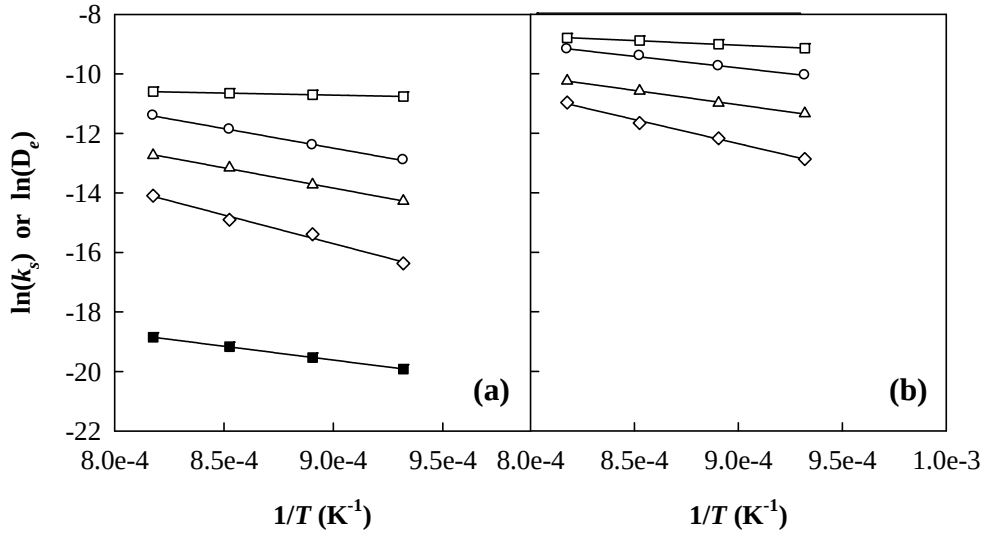


Fig. 12. Arrhenius plot for the kinetic constant $k_s$ for the reaction of $H_2$, CO, $CH_4$ and $O_2$ and the effective diffusivity, $D_e$, for the oxidation with (a) pre-oxidized and (b) activated ilmenite. $k_s$: ° $H_2$; △ CO; ◇ $CH_4$; □ $O_2$. $D_s$: ■ $O_2$

Reaction Kinetics of Ilmenite for Chemical-Looping Combustion.
Alberto Abad, Juan Adánez, Ana Cuadrat, Francisco García-Labiano, Pilar Gayán, and Luis F. de Diego.

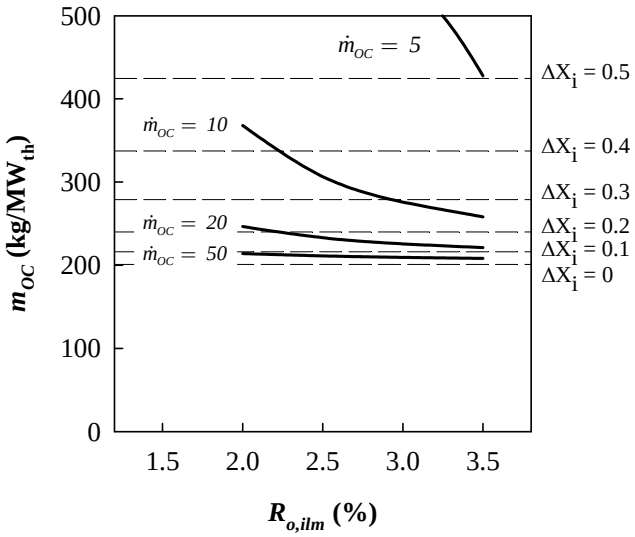


Fig. 13. Solids inventory for activated ilmenite (kg of solids per $MW_{th}$ of fuel) as a function of the oxygen transport capacity for several solids circulation flow-rate, $\dot{m}_{OC}$ (kg $s^{-1}$ per $MW_{th}$). $T$ = 1223 K; $X_{i,in}$ = 0.5-$\Delta X_i$/2.

**Captions of Tables**

Table 1. Composition (wt.%) and physical properties of pre-oxidized and activated ilmenite.

Table 2. Kinetic parameters for ilmenite reduction with $H_2$, CO and $CH_4$, and oxidation with air.

Table 3. Minimum solid inventory data for pre-oxidized and activated ilmenite (kg of solids per $MW_{th}$ of fuel).

Table 1. Composition (wt.%) and physical properties of pre-oxidized and activated ilmenite.

| | **Pre-oxidized ilmenite** | **Activated ilmenite** |
|---|---|---|
| XRD (main species) | $Fe_2TiO_5$, $Fe_2O_3$, $TiO_2$ | $Fe_2TiO_5$, $Fe_2O_3$, $TiO_2$ |
| $Fe_2O_3$ | 11.2 | 22.0 |
| $Fe_2TiO_5$ | 54.7 | 38.5 |
| $TiO_2$ | 28.6 | 34.0 |
| Inerts | 5.5 | 5.5 |
| True density ($kg/m^3$) | 4100 | 4250 |
| $R_{o,ilm}$ (%) | 4.0 | 3.3 |
| Grain radius, $r_g$ (μm) | 0.5 | 1.25 |
| Porosity (%) | 1.2 | 12.7 |
| BET Surface ($m^2/g$) | 0.8 | 0.4 |
| Crushing strength (N) | 2.2 | 2.0 |

Table 2. Kinetic parameters for ilmenite reduction with $H_2$, CO and $CH_4$, and oxidation with air.

| **Kinetic parameters** | **Pre-oxidized** | | | | **Activated** | | | |
|---|---|---|---|---|---|---|---|---|
| | $H_2$ | CO | $CH_4$ | $O_2$ | $H_2$ | CO | $CH_4$ | $O_2$ |
| $\rho_m$ (mol/m$^3$) | 13590 | 13590 | 13590 | 31100 | 13590 | 13590 | 13590 | 31100 |
| $r_g$ (m) | $0.5\ 10^{-6}$ | $0.5\ 10^{-6}$ | $0.5\ 10^{-6}$ | $0.48\ 10^{-6}$ | $1.25\ 10^{-6}$ | $1.25\ 10^{-6}$ | $1.25\ 10^{-6}$ | $1.20\ 10^{-6}$ |
| $\bar{b}$ | 1.19 | 1.19 | 4.74 | 4 | 1.45 | 1.45 | 5.78 | 4 |
| $k_{s0}$ (mol$^{1-n}$ m$^{3n-2}$ s$^{-1}$) | $5.1\ 10^{-1}$ | $2.1\ 10^{-1}$ | 8.8 | $8.0\cdot10^{-5}$ | $6.2\cdot10^{-2}$ | $1.0\cdot10^{-1}$ | 9.8 | $1.9\cdot10^{-3}$ |
| $E_{chr}$ (kJ/mol) | 109.2±2.3 | 113.3±3.0 | 165.2±12.4 | 11.8±0.1 | 65.0±2.7 | 80.7±2.4 | 135.2±6.6 | 25.5±1.2 |
| $n$ | 1 | 1 | 1 | 1 | 1 | 0.8 | 1 | 1 |
| $D_{e0}$ (mol m$^{-2}$ s$^{-1}$) | | | | $1.37\cdot10^{-5}$ | | | | |
| $E_{dif}$ (kJ/mol) | | | | 77.4±0.3 | | | | |

Table 3. Minimum solid inventory data for pre-oxidized and activated ilmenite (kg of solids per $MW_{th}$ of fuel).

| | Pre-oxidized | | | | Activated | | | |
|---|---|---|---|---|---|---|---|---|
| Fuel Reactor | $H_2$ | CO | $CH_4$ | Coal[(1)] | $H_2$ | CO | $CH_4$ | Coal[(1)] |
| $\overline{C}_g$ (% of fuel) | 14.5 | 14.5 | 5.3 | 5 | 14.5 | 19.2 | 5.3 | 5 |
| $T$ = 1173 K | 299 | 955 | 4481 | 1152 | 66 | 189 | 461 | 253 |
| $T$ = 1223 K | 197 | 619 | 2337 | 760 | 52 | 139 | 272 | 201 |
| $T$ = 1273 K | 135 | 416 | 1285 | 519 | 42 | 105 | 167 | 163 |
| Air Reactor[(2)] | $H_2$ | CO | $CH_4$ | Coal | $H_2$ | CO | $CH_4$ | Coal |
| $T$ = 1173 K | 75 | 64 | 90 | 99 | 39 | 33 | 47 | 52 |
| $T$ = 1223 K | 74 | 63 | 89 | 99 | 37 | 31 | 44 | 49 |
| $T$ = 1273 K | 74 | 63 | 89 | 98 | 35 | 30 | 42 | 46 |

(1) It was used 5 vol% $H_2$ for coal as fuel

(2) The reaction rate was calculated using 11.1 vol% $O_2$